To the Graduate Council:

I am submitting herewith a thesis written by Penny McFarlan Masuoka entitled "Analysis of Photogeologic Fracture Traces and Lineaments in the Northern Portion of the Wartburg Basin, Tennessee." I have examined the final copy of this thesis for form and content and recommend that it be accepted in partial fulfillment of the requirements for the degree of Master of Science, with a major in Geology.

G. Michael Clark

G. Michael Clark, Major Professor

We have read this thesis and recommend its acceptance:

Don A. Byerly

John B. Rehder

Accepted for the Council:

Vice Chancellor
Graduate Studies and Research

ANALYSIS OF PHOTOGEOLOGIC FRACTURE TRACES AND LINEAMENTS IN THE NORTHERN PORTION OF THE WARTBURG BASIN, TENNESSEE

A Thesis

Presented for the

Master of Science

Degree

The University of Tennessee, Knoxville

Penny McFarlan Masuoka

June 1981

3055394

ACKNOWLEDGMENTS

The writer is indebted to the professors who served on the committee for this thesis, Drs. G. Michael Clark, Don W. Byerly and J. B. Rehder. Dr. Robert Belcher and Dr. Herbert Blodget, NASA Goddard Space Flight Center, made useful suggestions during this study. The Geological Society of America provided partial funding for this thesis. The writer also acknowledges The University of Tennessee Computing Center, Knoxville, whose facilities were used to obtain some of the statistical data presented in this thesis. Edward Masuoka acted as field assistant and gave advice on debugging computer programs used in this study. Sue McFarlan typed the first draft of this thesis. Charles Glazzard assisted in the sediment analysis.

ABSTRACT

Photogeologic fracture trace and lineament mapping and analysis in the Wartburg Basin reveals important new information on the nature of fracturing in this area.

Fracture traces and lineaments were mapped on ASCS black and white panchromatic aerial photographs and NASA high altitude color infrared imagery. To check the accuracy of the linear feature map, bedrock joint orientations measured at eighteen field sites were compared to histograms of photogeologic linear feature orientations surrounding each site. Similarities were found to exist between a number of the histograms. Dissimilar histograms were probably a result of either limited bedrock exposure or low photogeologic fracture density for that area.

Examples of alignments in soils, vegetation and topographic-erosional features were examined in the field. The soil fracture trace was composed of a dark alignment of soil with a dark green, lush vegetation covering. The alignment of vegetation consisted of a line of moisture-loving, dark-colored hemlock trees, probably due to groundwater seepage associated with a zone of bedrock fractures. For field sites containing erosional alignments which crossed bedrock exposures, strike maxima of bedrock joint histograms corresponded closely to the orientation of the photogeologic linear features.

The photogeologic linear feature map was analyzed by contouring fracture frequency (similar to fracture density) for two quadrangles. A comparison of the fracture frequency maps to geologic maps shows

that, in general, photogeologic fracture density increases on the flanks and noses of folds where maximum folding has occurred. Fracture density was the lowest in areas where extensive strip mining and alluvium have obscured the photogeologic linear features.

To summarize the orientation data, histograms of lineament and fracture trace orientations were drawn across the study area. Using local fold axes in the eastern part of the study area as a reference, fractures appear to have originated from both tension and shear stress with tension fractures forming the largest class.

Data collected during this study indicate that photogeologic linear features can be used in this area not only for locating zones of increased fracture density reflected by individual fracture traces but also for locating local gentle folds. In unmapped areas of the Wartburg Basin, this technique might be useful for locating oil-bearing structures.

TABLE OF CONTENTS

CHAPTER		PAGE
I.	INTRODUCTION	1
	General Statement	1
	Previous Investigations	1
	Purpose	3
II.	THE STUDY AREA	5
	Location	5
	Stratigraphy	6
	Structure	7
III.	COLLECTION OF PHOTOGEOLOGIC DATA	11
	Definitions	11
	Imagery of the Study Area	12
	Equipment and Materials Used	15
	Procedure	16
	Summary of Photogeologic Data	18
IV.	COLLECTION OF FIELD DATA	19
	Introduction	19
	Selection of Field Sites	19
	Procedure	20
	Summary of Field Data	22
V.	VALIDITY OF FRACTURE TRACE AND LINEAMENT MAP	24
	Introduction	24
	Comparison of Photogeologic Linear Feature Orientations and Bedrock Joint Orientations	24
	Examples of Linear Features in the Field	25
	Operator Consistency	35
VI.	ANALYSIS AND INTERPRETATION OF THE PHOTOGEOLOGIC LINEAR FEATURE MAP	39
	Introduction	39
	Effects of Lithology on Photogeologic Fracture Density	40
	Effects of Local Structure on Fracture Density	42
	Lineament and Fracture Trace Orientations Across the Wartburg Basin	47

CHAPTER PAGE

VII. CONCLUSIONS 51

LIST OF REFERENCES 54

APPENDICES 61

A. COMPUTER PROGRAM TO DRAW ROSE DIAGRAMS 62

B. HISTOGRAMS OF PHOTOGEOLOGIC LINEAR FEATURES AND BEDROCK JOINTS 68

C. SUMMARY OF PHOTOGEOLOGIC DATA 87

VITA 91

LIST OF TABLES

TABLE		PAGE
1.	Government Agencies and Private Companies which Hold Aerial Photography and Imagery of the Wartburg Basin, Tennessee	13
2.	Aerial Photography Used to Map Lineaments and Fracture Traces for this Study	14
3.	Comparison of Fractures Measured in this Investigation and in the Investigation by Slusarski (1979)	23
4.	Demonstration of Operator Consistency by Repetitive Drawing of Lineaments and Fracture Traces on Three Photographs on Three Separate Dates	38
5.	A Comparison of Fracture Density for Four Formations in Ketchen Quadrangle	43

LIST OF FIGURES

FIGURE		PAGE
1.	Location of the Project Area (After Wilson et al., 1956)	2
2.	Stratigraphic Column in the Wartburg Basin (After Luther, 1959)	8
3.	Revisions in Nomenclature Proposed by Barlow (1969)	9
4.	Chart used to Record Lineament and Fracture Trace Data (from Slusarski, 1979)	17
5.	Location of Field Sites A-S	21
6.	Aerial Photograph Showing Soil Fracture Trace at Site M	27
7.	Photograph of Soil Samples B and D	28
8.	Histogram of Size Distribution of Soil Samples A and B from Site M	29
9.	Histogram of Size Distribution of Soil Samples C and D Taken from Site M	30
10.	Aerial Photograph of Dark Vegetation Alignment at Site H	32
11.	Histogram of Bedrock Joint Orientations for Site H with the Orientations of Fracture Trace Numbers 115 and 116 Shown	33
12.	Histogram of Bedrock Joint Orientations for Site C with the Orientation of Fracture Trace Number 4 Falling within the Largest Class	34
13.	Histogram of Bedrock Joint Orientations for Site F with the Orientation of Fracture Trace Number H109 Falling within the Largest Class	36
14.	Histogram of Bedrock Joint Orientations for Site P with the Orientation of Fracture Trace Number 955 Shown	37
15.	Geologic and Fracture Trace Map of Southwest Corner of Ketchen Quadrangle	41

FIGURE PAGE

16. Fracture Frequency Map Superimposed on a Structure Contour Map of Ketchen Quadrangle 45

17. Fracture Frequency Map Superimposed on a Structure Contour Map of Jellico West Quadrangle 46

18. Rose Diagrams for Lineaments and Fracture Traces across the Wartburg Basin 48

19. A Comparison of the Rose Diagrams from the Eastern Side of the Wartburg Basin to the Idealized Joint Distribution Associated with Folding 49

B-1. Histogram of Photogeologic Linear Feature Orientations which Lie within One Mile of Site A and Histogram of Joint Orientations from Field Site A 69

B-2. Histogram of Photogeologic Linear Feature Orientations which Lie within One Mile of Site B and Histogram of Joint Orientations from Field Site B 70

B-3. Histogram of Photogeologic Linear Feature Orientations which Lie within One mile of Site C and Histogram of Joint Orientations from Field Site C 71

B-4. Histogram of Photogeologic Linear Feature Orientations which Lie within 1.5 Miles of Site D and Histogram of Joint Orientations from Field Site D 72

B-5. Histogram of Photogeologic Linear Feature Orientations which Lie within 1.25 Miles of Site E and Histogram of Joint Orientations from Field Site E 73

B-6. Histogram of Photogeologic Linear Feature Orientations which Lie within One Mile of Site F and Histogram of Joint Orientations from Field Site F 74

B-7. Histogram of Photogeologic Linear Feature Orientations which Lie within One Mile of Site G and Histogram of Joint Orientations from Field Site G 75

B-8. Histogram of Photogeologic Linear Feature Orientations which Lie within One Mile of Site H and Histogram of Joint Orientations from Field Site H 76

FIGURE PAGE

B-9. Histogram of Photogeologic Linear Feature Orientations which Lie within One Mile of Site I and Histogram of Joint Orientations from Field Site I 77

B-10. Histogram of Photogeologic Linear Feature Orientations which Lie within 1.25 Miles of Site J and Histogram of Joint Orientations from Field Site J 78

B-11. Histogram of Photogeologic Linear Feature Orientations which Lie within 1.5 Miles of Site K and Histogram of Joint Orientations from Field Site K 79

B-12. Histogram of Photogeologic Linear Feature Orientations which Lie within 1.5 Miles of Site L and Histogram of Joint Orientations from Field Site L 80

B-13. Histogram of Photogeologic Linear Feature Orientations which Lie within One Mile of Site N and Histogram of Joint Orientations from Field Site N 81

B-14. Histogram of Photogeologic Linear Feature Orientations which Lie within One Mile of Site O and Histogram of Joint Orientations from Field Site O 82

B-15. Histogram of Photogeologic Linear Feature Orientations which Lie within 1.5 Miles of Site P and Histogram of Joint Orientations from Field Site P 83

B-16. Histogram of Photogeologic Linear Feature Orientations which Lie within 1.5 Miles of Site Q and Histogram of Joint Orientations from Field Site Q 84

B-17. Histogram of Photogeologic Linear Feature Orientations which Lie within One Mile of Site R and Histogram of Joint Orientations from Field Site R 85

B-18. Histogram of Photogeologic Linear Feature Orientations which Lie within 1.5 Miles of Site S and Histogram of Joint Orientations from Field Site S 86

LIST OF PLATES

PLATE

I. Photogeologic Fracture Traces and Lineaments in the Wartburg Basin . . . . . IN POCKET

CHAPTER I

INTRODUCTION

General Statement

Photogeologic lineaments and fracture traces are noncultural linear features consisting of topographic, soil color, or vegetation alignments which can be mapped on remotely sensed imagery (Lattman, 1958). Because they are thought to represent fractures or zones of increased fracturing, photogeologic linear features are useful tools for studying the geology of an area. Over the years, photogeologic linear features have been used for a wide variety of investigations such as: petroleum exploration (Blanchet, 1957), groundwater hydrology (Moore et al., 1975), and mineralization (Moore and Hollyday, 1976). Photogeologic linear features have also been used in regional tectonic studies (Gold et al., 1973; Gol'braikh et al., 1968).

This paper is primarily concerned with lineaments and fracture traces of the northern portion of the Wartburg Basin, Tennessee (Figure 1), and their relationship to the local structural geology of that area.

Previous Investigations

In 1911, Hobbs recognized a world wide fracturing pattern from the analysis of drainage lines. Hobbs called these lines "lineaments—significant lines in the earth's surface."

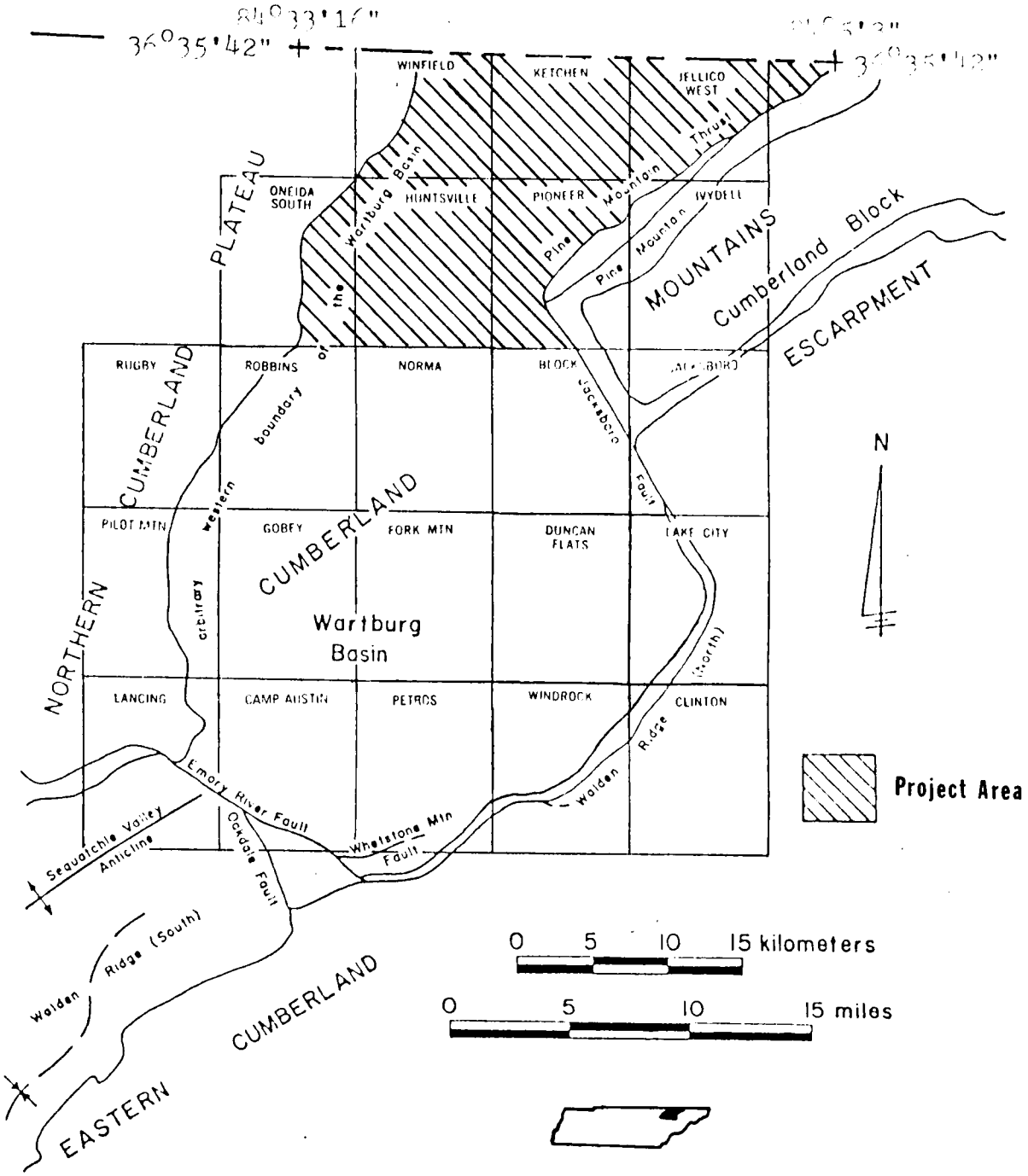


Figure 1. Location of the project area (after Wilson et al., 1956).

Kaiser (1950) observed that lineaments are associated with zones of closely-spaced joints. He also noted that lineaments are often associated with minor changes in strike of sedimentary beds. Kaiser defined lineament as:

> A straight linear feature that is at least many hundreds of feet and commonly many miles long. Lineaments are well shown on aerial photographs and may consist of (1) linear topographic features, either trenches or ridges; (2) linear vegetation patterns; or (3) linear patterns of soil color or texture.

In 1957, Blanchet detailed the steps of a photogeologic fracture analysis including instructions for: mapping lineaments on aerial photographs, drawing azimuth frequency diagrams, and drawing a "fracture-incidence map" which shows the number of fracture traces per unit area.

Slusarski (1979) compiled a lineament and fracture trace map in an area of the Wartburg Basin to the south of this thesis study area. Slusarski found similarities of strike maxima between photogeologic linear features and bedrock fractures. He concluded that although the bedrock for most of the Wartburg Basin is obscured by soil and dense vegetation, photogeologic mapping can be used to interpret bedrock structures. As far as this author could determine, no other photogeologic fracture analysis has been completed for the Wartburg Basin, Tennessee.

Purpose

The objectives of this study are: first, to compile a photogeologic linear feature map of the northern portion of the Wartburg Basin;

second, to determine if photogeologic linear features drawn by this author reflect bedrock structural elements; third, to determine how lineament and fracture trace orientations might change across the basin; and fourth, to determine how the linear feature frequency distribution changes in relation to lithology and structural geology of the area.

In order to complete these goals, the project was divided into four phases. The first phase consisted of mapping lineaments and fracture traces on aerial photographs and transferring them to topographic quadrangle maps. During the second phase, bedrock joints were measured and photogeologic linear features were studied for nineteen field sites. The third phase consisted of comparing the strike of bedrock joints with the orientations of photogeologic linear features by means of circular histograms. Also, operator consistency was checked by repetitive mapping of linear features for three photographs. The fourth phase involved the interpretation of the linear feature map. Two methods were used to summarize the data on the map: rose diagrams of linear feature orientations drawn at intervals across the map and a contour map of lineament and fracture trace frequency drawn for two of the topographic quadrangles.

CHAPTER II

THE STUDY AREA

Location

The study area is the northern portion of the Wartburg Basin, Tennessee (Figure 1). The area includes part of both Scott and Campbell Counties. Parts of the following eight topographic quadrangles are included in this study: Winfield, Ketchen, Jellico West, Jellico East, Oneida South, Huntsville, Pioneer, and Ivydell. The total project area covers approximately 239 square miles (619 square kilometers).

The Wartburg Basin is a subprovince of the Cumberland Plateau Physiographic Province. It is bounded by the Jacksboro and Pine Mountain Faults on the northeast, by Walden Ridge on the southeast, and by the Emory River and Whetstone Mountain Faults on the southwest (Wilson et al., 1956). The western boundary of the Wartburg Basin has, at present, been defined arbitrarily (Wilson et al., 1956) as shown in Figure 1. During the course of this investigation, the author could find no evidence to dispute this arbitrary boundary. However, within the study area, there does appear to be a gradual change in the terrain, from the Wartburg Basin to the adjacent Northern Cumberland Plateau. Therefore, a physiographic boundary based on a complete terrain analysis (using altitude, relief, dominant geology, drainage pattern, characteristic plan-profile, and so on) would

probably prove to be superior to the present arbitrary boundary (Ollier, 1977; Van Lopik and Kolb, 1959). However, such a terrain analysis is far beyond the scope of this study. For this reason, the arbitrary boundary drawn by Wilson et al. (1956) is used as the western edge of the research area.

There were several reasons for selecting this area for a lineament and fracture trace study. Tennessee has had few fracture trace and lineament studies; and, in the northern part of the Wartburg Basin, no such studies have been made as far as the author could determine. However, studies of lineament and fracture trace patterns are needed to assist the active petroleum exploration in this area. This particular area was chosen because it extends from the eastern boundary to the western boundary of the Basin; so that any changes in lineament and fracture trace orientation across the Basin could be noted. The final reason for selecting this area is that the Wartburg Basin is generally uniform in underlying stratigraphic units, vegetation, and relief. Therefore, changes in the lineament and fracture trace map are more likely to reflect changes in structural factors rather than changes in lithology, vegetation or terrain of the area.

Stratigraphy

The research area is underlain by Pennsylvanian age rocks consisting primarily of sandstone, shale, conglomerate, and coal. Several coal seams in this area are being actively mined. A generalized stratigraphic column of the Wartburg Basin is shown in

Figure 2 (after Luther, 1959). The Cross Mountain, Vowell Mountain, Red Oak Mountain, Graves Gap, Indian Bluff, Slatestone and Crooked Fork Groups constitute the major exposures in the research area (Wilson et al., 1956). Minor exposures of the Crab Orchard Mountains and Gizzard Groups have been exposed along the eastern edge of the study area by the Pine Mountain Thrust Fault.

Barlow (1969) proposed revisions in the nomenclature and placement of formation boundaries (Figure 3). The lower boundary of the Cross Mountain Group was extended down to the Upper Pioneer Coal so that it encompassed the former Cross Mountain Group, the Vowell Mountain Group, the Red Oak Mountain Group, and part of the Graves Gap Group. Boundaries of the Graves Gap Formation were changed to extend from the bottom of the Cross Mountain Group to the top of the Pioneer Sandstone.

Structure

The Wartburg Basin is a structural basin with the structurally lowest part located south of the research area where Scott, Campbell, Morgan and Anderson Counties meet (Luther, 1959). On the west side, the Wartburg Basin Subprovince merges with the Northern Cumberland Plateau Subprovince. Beds dip gently into the Basin from the west and south sides and dip more steeply into the Basin from the east (Luther, 1959).

The Pine Mountain and Jacksboro Faults bound the eastern side of the research area and are the major structures within the study area.

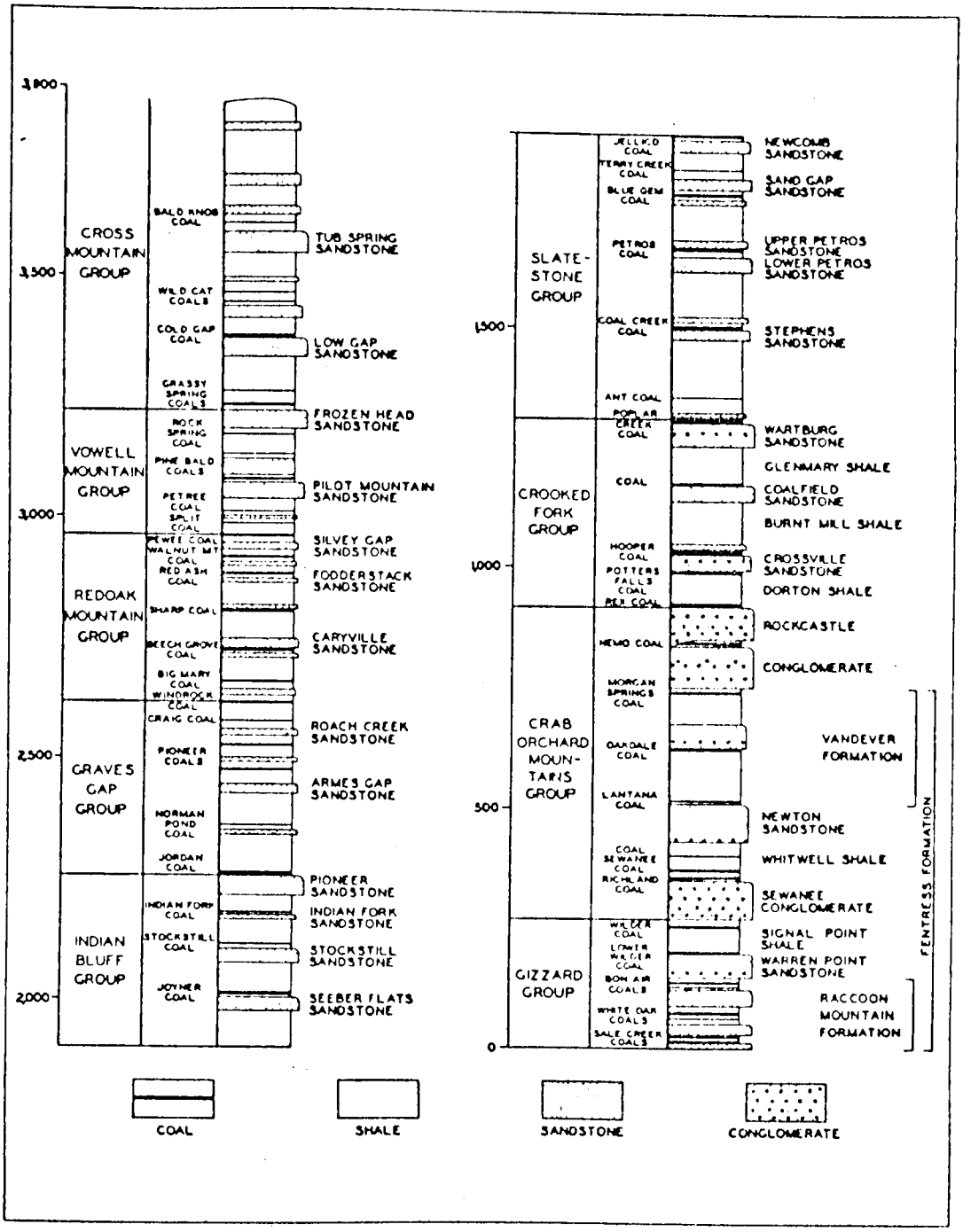


Figure 2. Stratigraphic column in the Wartburg Basin (after Luther, 1959).

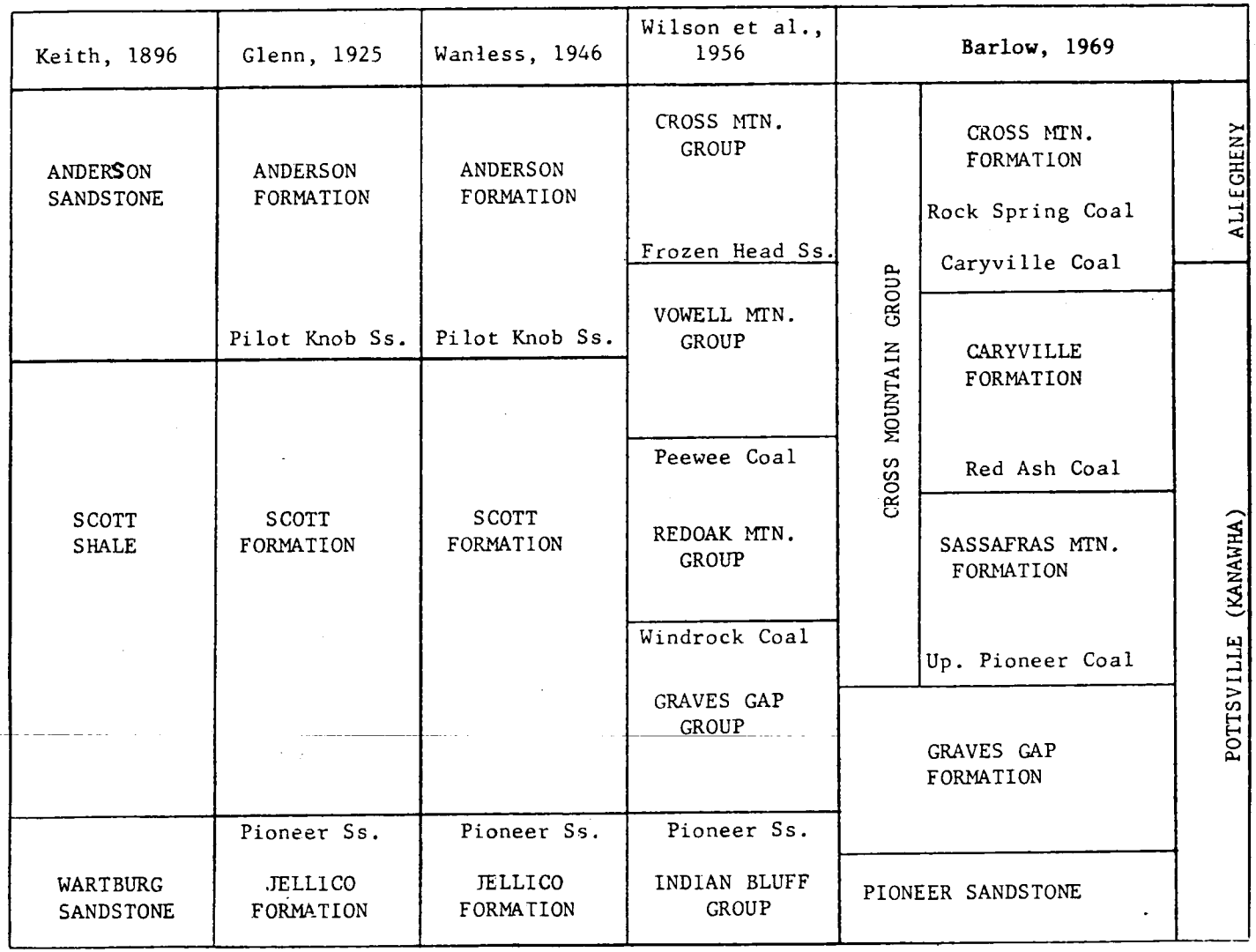


Figure 3. Revisions in nomenclature proposed by Barlow (1969).

The Pine Mountain Fault is a low angle thrust fault which moved the Cumberland Block of the Cumberland Plateau to the northwest. This fault is exposed in Elk Valley to the east of the study area as a fault zone consisting of several closely spaced faults that are thought to merge at depth (Luther, 1959). The Jacksboro Fault is a strike-slip fault along which the Cumberland Block moved to the northwest.

CHAPTER III

COLLECTION OF PHOTOGEOLOGIC DATA

Definitions

Hobbs, in 1904, defined lineaments as "the significant lines of landscape which reveal the hidden architecture of the rock basement." Since this early definition, the terms, lineament and fracture trace, have been redefined several times resulting in a large amount of confusion. This study will use the definitions proposed by Lattman (1958),

> A photogeologic fracture trace is a natural linear feature consisting of topographic (including straight stream segments), vegetation, or soil tonal alignments, visible primarily on aerial photographs, and expressed continuously for less than one mile. Only natural linear features not obviously related to outcrop pattern of tilted beds, lineation and foliation, and stratigraphic contacts are classified as fracture traces. Included in this term are joints mapped on aerial photographs where bare rock is observed.
>
> A photogeologic lineament is a natural linear feature consisting of topographic (including straight stream segments), vegetation, or soil tonal alignments, visible primarily on aerial photographs or mosaics, and expressed continuously or discontinuously for many miles. The restrictions placed on the term "fracture trace" as regards origin apply equally to the term "lineament."

By definition, the difference between lineaments and fracture traces is based on length. The division is arbitrarily chosen at one mile. Lattman gave several reasons for this division. The term, lineament, already had the connotation of being a long feature. Also, when the definitions were proposed, a different technique was

used to map lineaments. Lineaments were mapped on photo mosaics; whereas fracture traces were mapped on individual aerial photographs. (Today, however, lineaments are often mapped on high altitude or satellite imagery.) Finally, Lattman found that fracture traces are more likely to represent bedrock joints or small scale faults and lineaments are more likely to be large scale faults.

This chapter concerns the process of mapping lineaments and fracture traces within the study area.

Imagery of the Study Area

Table 1 lists the various sources of the imagery that is currently available for the Wartburg Basin. SEASAT, radar satellite imagery, though not available to the public at this time, should soon become available presumably through the EROS Data Center. As far as the writer could determine, the five agencies listed in Table 1, hold all imagery of the Wartburg Basin that would be available to the public.

Two types of aerial photography were chosen to cover the study area, ASCS black and white panchromatic aerial photography and NASA high altitude color infrared photography (see Table 2). Each set completely covers the entire study area. Using different kinds of photography (different dates, scales, etc.) for separate parts of the linear map could cause a variation in the lineament pattern unrelated to the structure of the region. For this reason, only two types of photography, each completely covering the study area, were selected.

TABLE 1

GOVERNMENT AGENCIES AND PRIVATE COMPANIES WHICH HOLD AERIAL PHOTOGRAPHY AND IMAGERY OF THE WARTBURG BASIN, TENNESSEE

Agency	Address of Agency	Type of Imagery	Date of Imagery	Scale of Print	Area of Wartburg Basin Covered
Agricultural Stabilization and Conservation Service (ASCS) Aerial Photography Field Office	2222 West, 2300 South P. O. Box 30010 Salt Lake City, Utah 84125	Black and White Panchromatic	October 1973	1:20,000	Total Coverage
National Aeronautics and Space Administration (NASA) EROS Data Center	EROS Data Center Sioux Falls, SD 57198	Lansat Multispectral Scanner	Various	1:500,000	Total Coverage
		Hyper-Altitude Color IR, Color	Various	Various	Total Coverage
Tennessee Valley Authority (TVA) Map Sales Division	Map Sales Division 200 Haney Building Chattanooga, Tennessee 37401	Black and White Panchromatic	Various	Various	Total Coverage of Wartburg Basin but at various scales and dates.
Tennessee Department of Transportation Aerial Surveys Division	Gun Club Lane Metro Airport Nashville, Tennessee 37217	Black and White Panchromatic	May 1966	1:24,000	Total Coverage of Scott, Morgan and Anderson Counties. Partial Coverage of Campbell County.
Continental Aerial Surveys, Inc.	Singleton Station Road Alcoa, Tennessee	Black and White Panchromatic	March 1976	1:72,000	Total Coverage of all quadrangles except Winfield, Ketchen, Jellico West, Jellico East, Rugby, Pilot Mtn., Lancing.

TABLE 2

AERIAL PHOTOGRAPHY USED TO MAP LINEAMENTS AND FRACTURE TRACES FOR THIS STUDY

Source	Type of Imagery	Date of Imagery	Image Size	Scale
National Aeronautics and Space Administration (NASA) EROS Data Center	Hyper-Altitude Color IR	April 1972	9 in. × 9 in. 22.9 cm. × 22.9 cm.	1:120,000
Agricultural Stabilization and Conservation Service (ASCS) Aerial Photography Field Office	Black and White Panchromatic	October 1973	9 in. × 9 in. 22.9 cm. × 22.9 cm.	1:20,000

The ASCS black and white photographs were selected because of their low cost and good quality, complete, stereoscopic coverage of the entire study area. Photographs held by the Department of Transportation do not provide total coverage of the study area. TVA has complete coverage but at various dates and scales. The stereoscopic coverage provided by the ASCS photography was an important factor in its selection because stereoscopic viewing allows identification of subtle topographic depressions which characterizes some fracture traces.

NASA high altitude color infrared imagery was chosen to supplement the ASCS photography. Although the larger scale ASCS photography was excellent for mapping fracture traces, it was desirable to obtain small scale imagery that would allow the larger lineaments to be more easily mapped. The NASA high altitude photography is excellent for this; the entire thesis area is stereoscopically covered by five photographs. And, the low number of photographs allow complete coverage for a relatively low price. Finally, color infrared photography was chosen because it is useful for mapping lineaments expressed by vegetation alignments.

Equipment and Materials Used

Apart from the imagery used, relatively small amounts of equipment and materials were needed to map the lineaments and fracture traces in the study area. Clear acetate overlays were taped to every other photograph. Lineaments and fracture traces were traced directly on

the acetate with waterproof ink. Two stereoscopes were used, a pocket stereoscope (2x) and a scanning mirror stereoscope (1.5x and 4.5x). Topographic quadrangle maps at a scale of 1:24,000 were used for base maps. A protractor and an engineer's scale were used to measure the azimuth, length and width of each linear feature.

Procedure

A procedure involving eight steps was used to map lineaments and fracture traces from ASCS black and white photographs:

1. Photographs were trimmed and every other photograph was covered with a clear acetate overlay.
2. Photographs were arranged and filed by flight lines.
3. Lineaments and fracture traces were drawn on the overlays first by monoscopic examination, then by stereoscopic viewing (pocket stereoscope, then mirror stereoscope).
4. All photographs were compared to adjacent photographs to eliminate double annotation of a lineament due to photographic overlap.
5. Lineaments and fracture traces were numbered.
6. The chart shown in Figure 4 (Slusarski, 1979) was filled out, except for the columns labelled length and orientation.
7. Lineaments and fracture traces were transferred to topographic maps by inspection.
8. Orientation and length of each linear feature were measured from the topographic map.

PHOTOINTERPRETIVE FRACTURE TRACE AND LINEAMENT DATA																	
IMAGE NO.	EMULSION TYPE			FRACTURE TRACE NO.	COMPOSITION		PHOTOGEOLOGIC LINEAR EXPRESSION ELEMENTS					CONTINUITY		FRACTURE TRACE PARAMETERS		
	NORMAL B&W PANCHROMATIC	B&W I.R.	COLOR I.R.		SINGLE PHOTOINTERPRETIVE ELEMENT	MULTIPLE PHOTOINTERPRETIVE ELEMENTS	SOIL TONAL ALIGNMENT	VEGETATIONAL ALIGNMENT	TOPOGRAPHIC—EROSIONAL ALIGNMENTS		REMARKS	CONTINUOUS LINEAR ELEMENT(S)	SUBCONTINUOUS LINEAR ELEMENT(S)	MAPPABLE LENGTH	MAPPABLE WIDTH	ORIENTATION
									STREAM SEGMENT ALIGNMENTS	VALLEY OR RIDGE AXES ALIGNMENTS						

Figure 4. Chart used to record lineament and fracture trace data (from Slusarski, 1979).

This same procedure was uniformly followed for each photograph to provide some objectivity across the map. Thus, variations in the linear feature pattern are hopefully due to changes in the fracture pattern of the area rather than changes in the methods of observation.

The procedure for mapping lineaments on the NASA high altitude infrared photographs was almost the same as the steps outlined above. However, a pocket stereoscope was not used because these images were positive transparencies which do not permit the overlap needed for use of the pocket stereoscope.

The final lineament and fracture trace map is shown in Plate I.

Summary of Photogeologic Data

Data gathered on all of the photogeologic linear features were tabulated and are summarized in Appendix C.

Soil fracture traces, on the ASCS photographs, appeared as dark lines cutting across fields. Alignments in vegetation consisted of either a line of higher standing trees or a line of darker vegetation. Topographic-erosional linear features, consisting of valley alignments or stream segment alignments, were the most numerous type of linear feature.

Soil features were not mapped on the NASA color infrared imagery. Linear features were either of topographic-erosional expression or topographic-erosional and vegetation expression. On the NASA imagery, thirty-three new linear features were mapped that had not been mapped on the ASCS photography.

CHAPTER IV

COLLECTION OF FIELD DATA

Introduction

Field work for this project was conducted during August and September of 1980 after the photogeologic linear feature mapping was completed. The purpose of the field research was to relate the bedrock fracture pattern to the photogeologic linear feature pattern. To accomplish this purpose, two types of field work were done. First, bedrock fracture orientations were measured across the study area at eighteen of the nineteen field localities. And, secondly, five specific examples of linear features were visited in order to study their surface expression and, where photogeologic fracture traces or lineaments intersected a bedrock exposure, to take measurements of joint orientations.

Selection of Field Sites

Field sites were chosen prior to the field work by inspecting the aerial photography for rock exposures. Several factors influenced the selection of the field sites. Few natural outcrops (because of dense vegetation and a deep regolith) limited the field sites, for the most part, to strip mine highwalls or roadcuts. Also, travel to some areas was difficult because of poor roads or lack of roads and rugged

topography. Thus, only those exposures which appeared accessible, either on aerial photography or topographic maps, were chosen.

Some field sites were selected where a lineament or fracture trace intersected a bedrock exposure. One locality was chosen in order to study an example of a vegetation alignment and another was selected to study a soil tone alignment.

Of the nineteen sites chosen, only one was inaccessible. However, a few localities did not have the bedrock exposure that was expected. The exposure was either too weathered to be used or had been covered by strip mine reclamation programs. For these sites, nearby, alternative sites were chosen. The locations of the actual sites used are shown in Figure 5.

Procedure

Eighteen of the nineteen field sites had bedrock exposures where joints could be measured. At each site, this information was recorded: (1) strike of fracture, (2) dip of fracture, (3) lithology in which fracture occurs, (4) width of fracture, (5) length of fracture, and (6) spacing between members of any joint sets that were present. Where the bedrock exposure was large, fractures were measured at twenty or thirty foot intervals along the length of the exposure.

Where a lineament or fracture trace intersected a bedrock exposure, the following were noted: (1) composition of the linear feature (type of vegetation, etc.), (2) width of the linear feature, and (3) effects on the bedrock through which the lineament passed, if the bedrock was exposed.

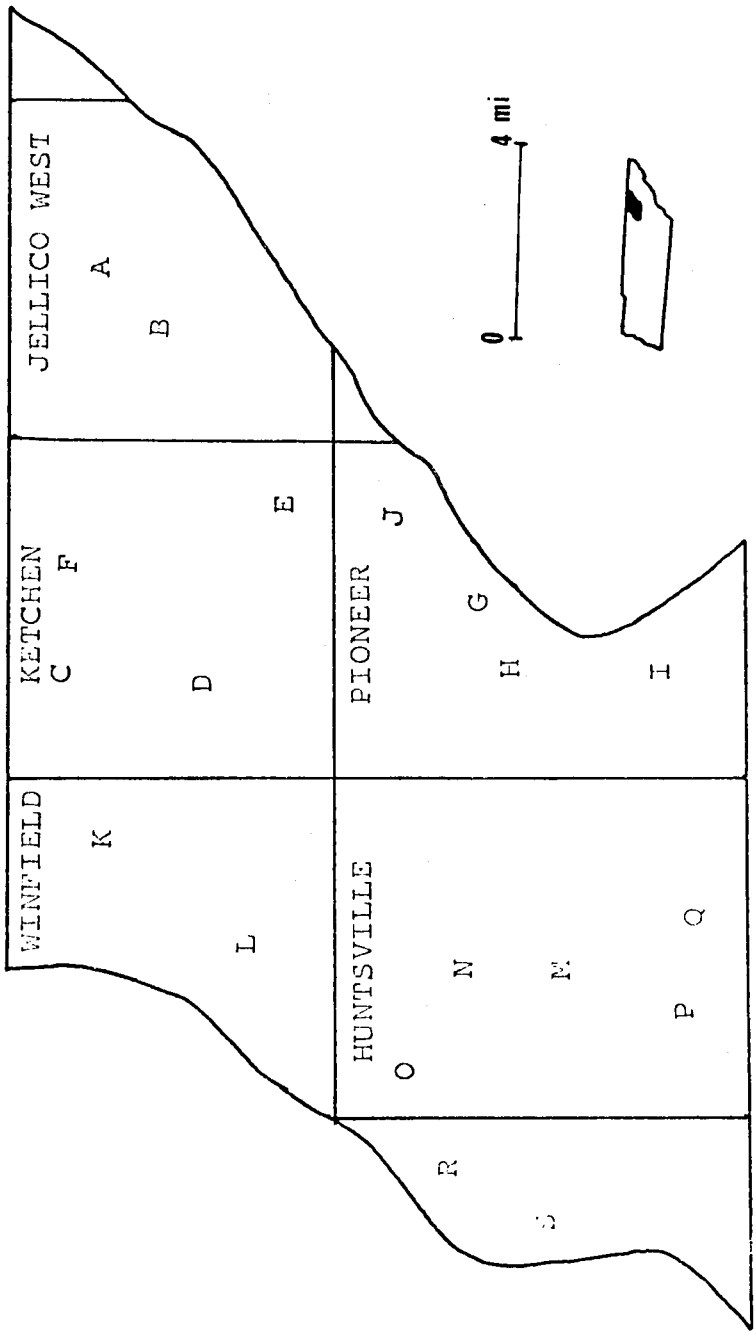


Figure 5. Location of field sites A-S.

Summary of Field Data

Fracture data from eighteen bedrock exposures, were summarized and evaluated in Table 3. Fractures measured in the research area were vertical or steeply dipping bedrock joints. No faults were seen or inferred in the field area. Most of the fractures measured were between one and ten feet (.304 and 3.04 meters) in height and had a width of one inch (2.54 centimeters) or less.

For the purpose of comparison, fracture data recorded by Slusarski (1979) in the southeastern portion of the Wartburg Basin, are presented in Table 3. The percentages for each dip interval measured in this study deviates from those measured by Slusarski by no more than 2%.

TABLE 3

COMPARISON OF FRACTURES MEASURED IN THIS INVESTIGATION AND IN THE INVESTIGATION BY SLUSARSKI (1979)

	This Investigation	Slusarski (1979)
Total Fractures Measured	473	193
Dip of Fractures		
90°-81°	311 (66%)	128 (66%)
80°-71°	125 (26%)	54 (28%)
71°	37 (8%)	11 (6%)
Lithology in Which Fractures Occur		
Sandstone	231 (49%)	72 (37%)
Siltstone	107 (23%)	40 (21%)
Shale	72 (15%)	39 (20%)
Sandstone-Shale	26 (6%)	29 (15%)
Sandstone-Siltstone	20 (16%)	0 (0%)
Shale-Siltstone	16 (3%)	0 (0%)
Coal	1 (<1%)	14 (7%)

CHAPTER V

VALIDITY OF FRACTURE TRACE AND LINEAMENT MAP

Introduction

Although some investigators have found good agreement between bedrock joint orientations and fracture trace and lineament orientations (Lattman and Nickelson, 1958; Alpay, 1973; Wobber, 1967; Boyer and McQueen, 1964); some studies have shown little or no agreement at all (Brown, 1961; Lattman and Matzke, 1961; Podwysocki, 1974b). It is very important in any lineament and fracture trace study to demonstrate how reliable the lineament and fracture trace map is.

In this project, the validity of the lineament and fracture trace map was tested in three ways: (1) by comparing the photogeologic linear feature orientations to bedrock joint orientations using circular histograms, (2) by studying field sites containing examples of linear features, and (3) by demonstrating operator consistency through repetitive linear feature mapping on three aerial photographs.

Comparison of Photogeologic Linear Feature Orientations and Bedrock Joint Orientations

An interactive computer program was written to draw rose diagrams on the Tektronix Interactive Digital Plotter for an input file of either azimuths or digitized end points. This program is listed in Appendix A.

Using this program, rose diagrams were drawn for bedrock joint orientations which fell within one mile (1.6 kilometers) of the field site. Because of the low frequency of linear features in some areas of the map, some rose diagrams were redrawn within 1.25 or 1.5 miles (2 or 2.4 kilometers) of the field site (see Appendix B).

A comparison of the two sets of rose diagrams shows some similarity between bedrock joint orientations and photogeologic linear feature orientations. Joint measurements at Sites D, F, I, O and R (Figures B-4, B-6, B-9, B-14, and B-17 are quite similar to the orientations of fracture traces and lineaments of those areas. However, some of the sites were only fairly similar. And, two sites, E and K (Figures B-5 and B-11), were totally dissimilar.

Two factors might have affected the correspondence between bedrock joint orientations and photogeologic linear feature orientations. A lack of large bedrock exposures in some areas, led to an insufficient number of joint measurements for some sites. Also, for a few areas, low frequency of fracture traces made comparison with joint orientations difficult. Reasons for low linear feature frequency for some areas will be discussed in the next chapter.

Examples of Linear Features in the Field

Five of the nineteen field sites contained examples of photogeologic linear features. Site M was chosen in order to study an example of a soil color fracture trace. Site H contained an example of a vegetation alignment and a topographic-erosional alignment. The three remaining sites, C, F and P, had examples of topographic-erosional alignments.

Site M—Laxton's Field, Huntsville Quadrangle

On ASCS black and white aerial photographs, the soil fracture trace at Site M appears as a dark line running across a field (Figure 6). Although there were other examples of soil fracture traces mapped within the research area, Site M, was the most prominent and continuous.

In the field, the fracture trace was an extremely gentle topographic depression with a cover of dark green, lush grass. The grass in the surrounding field was much lighter in color. Four soil samples were taken, Samples B and C from the fracture trace area, and Samples A and D from the surrounding area. As expected, Samples B and C were darker in color than Samples A and D (Figure 7).

Studies of fracture traces in Illinois, have shown that water moving toward fractured zones tend to concentrate clay or silt-sized particles in the zone and, thus, produce a darker linear feature (Wobber, 1967). The higher clay content, by holding moisture in the soil, encourages a lush, dark green vegetation cover which enhances the linear feature.

The four soil samples taken at Site M were sieved and the resulting histograms are shown in Figures 8 and 9. Unlike Wobber (1967), there is little difference in grain size in the four samples.

Site H—Sexton Mountain, Pioneer Quadrangle

Three fracture traces were studied at Site H. On the aerial photographs, Fracture Trace #116 is a dark vegetation alignment

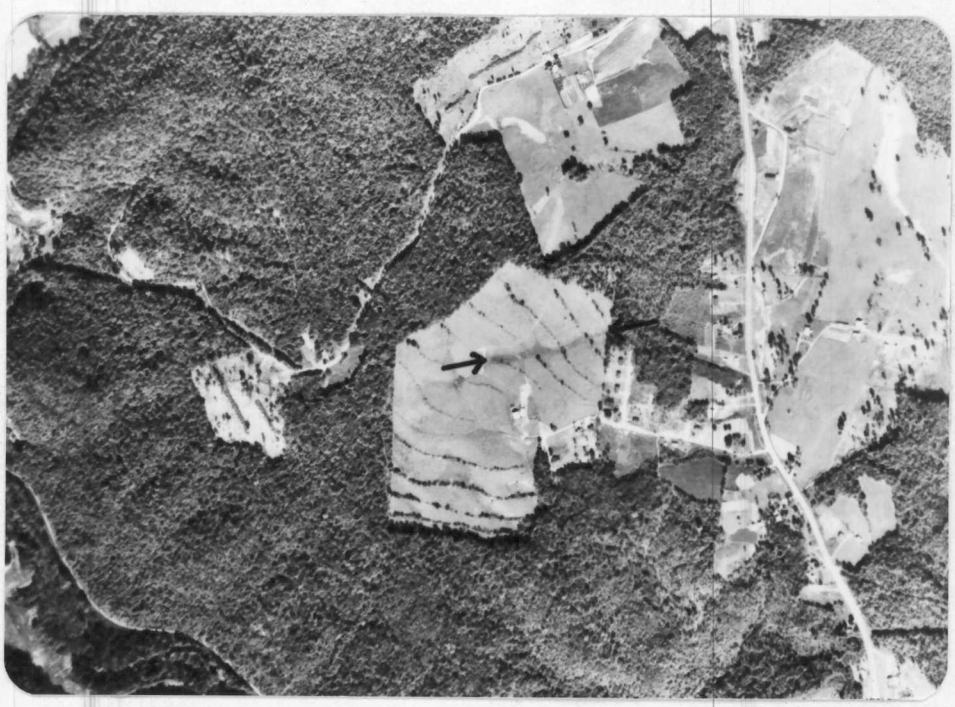


Figure 6. Aerial photograph showing soil fracture trace at Site M.

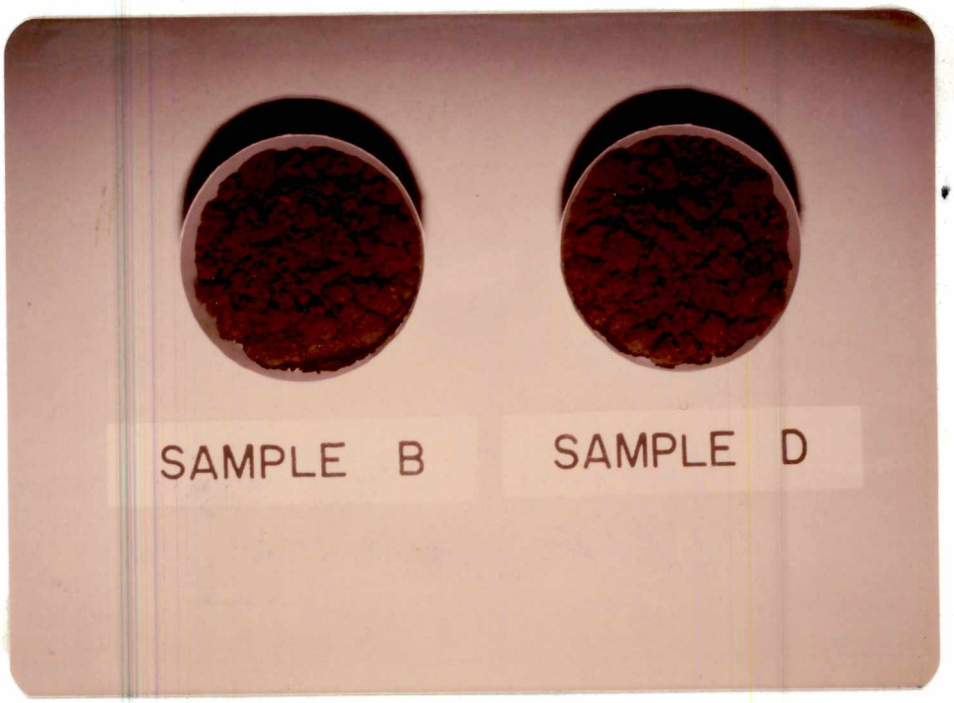


Figure 7. Photograph of soil samples B and D. The darker sample, B, was taken from the soil fracture trace at Site M.

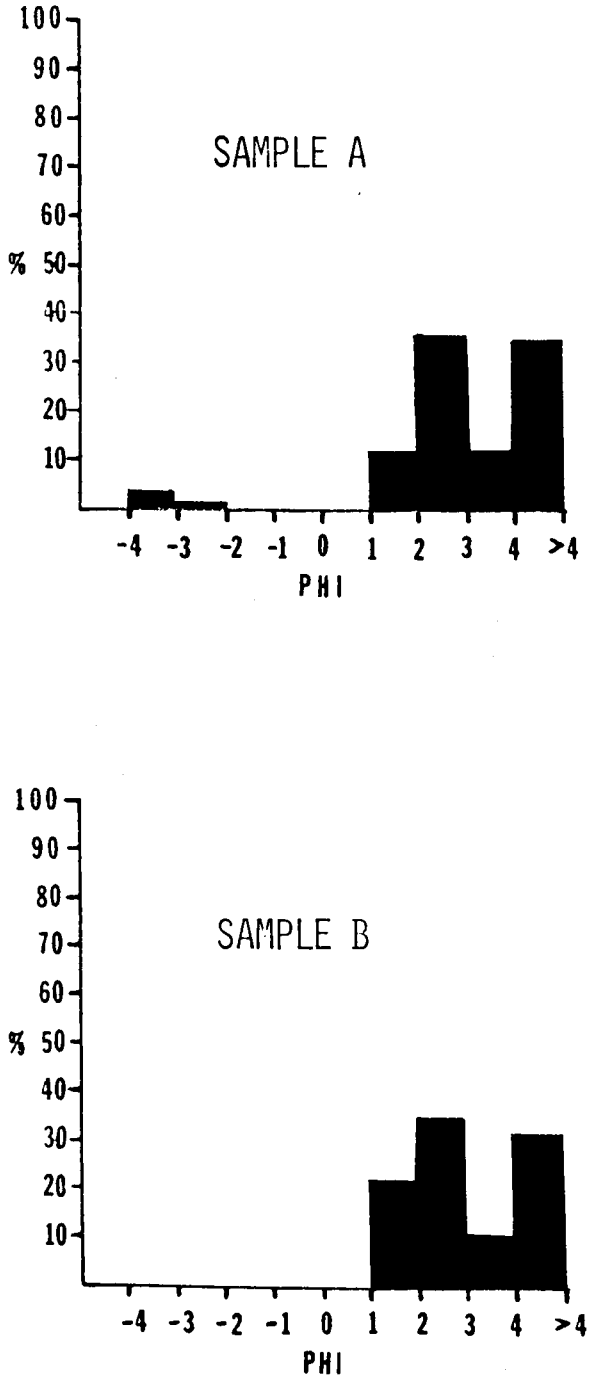


Figure 8. Histogram of size distribution of soil samples A and B from Site M. Sample B was taken from within the fracture trace.

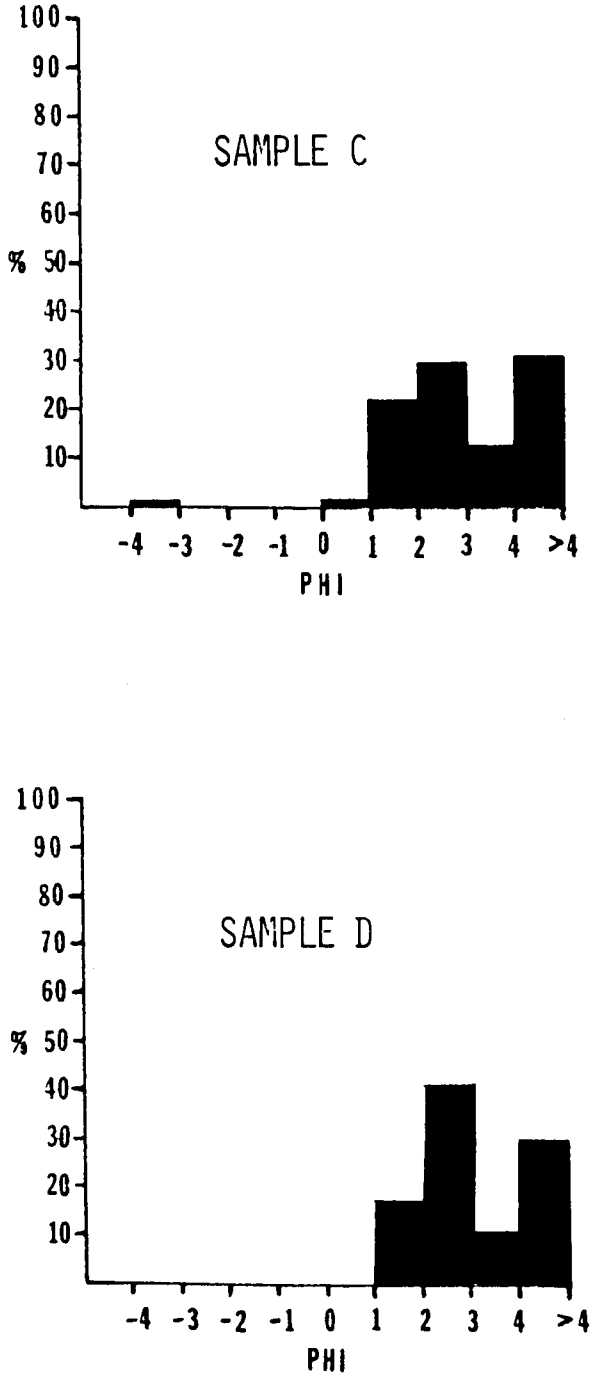


Figure 9. Histogram of size distribution of soil samples C and D taken from Site M. Sample C was taken from within the fracture trace.

(Figure 10). Fracture Trace #115 and #117 are topographic-erosional alignments.

In the field, Fracture Trace #116 consisted of a line of dark green Hemlock trees in a lighter deciduous forest. Since Hemlock trees grow in areas of increased soil moisture (Petrides, 1972), this vegetation alignment could be caused by groundwater seepage associated with a zone of bedrock fractures.

Fracture Trace #115 and #117 are extremely straight erosional alignments. A small bedrock outcrop was found where Fracture Traces #115 and #117 intersect. A histogram for the joint orientations for this outcrop with the orientations of the fracture traces, is shown in Figure 11.

Site C—Gum Fork, Ketchen Quadrangle

Site C is a strip mine highwall approximately thirty feet high. Three feet of sandstone caps shale beds. Fractures were measured mostly in the sandstone because the shale was highly weathered. Fracture Trace #4, a straight stream valley, intersects the northwest end of the outcrop. Figure 12 shows the orientation of Fracture Trace #4 plotted on a histogram of bedrock joint orientations. It falls within the largest class of the bedrock joint orientations.

Site F—Angel Gap, Ketchen Quadrangle

Site F is a strip mine highwall with about five feet of massive sandstone capping ten feet of silty shale. The outcrop was measured at twenty foot intervals. A fracture set with the attitude N327°/84°SW

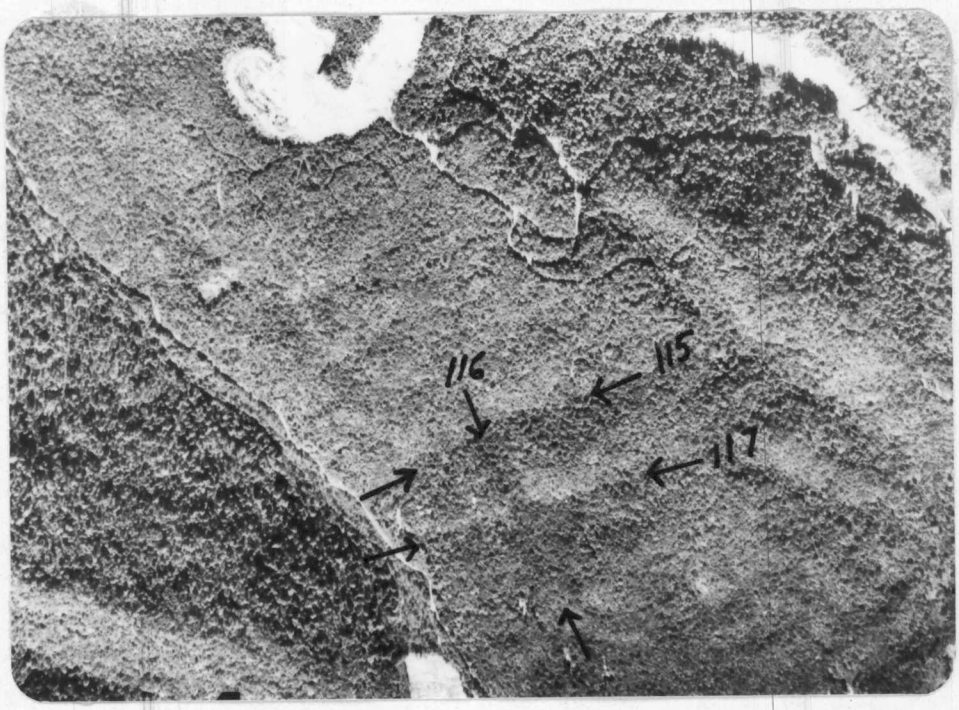


Figure 10. Aerial photograph of dark vegetation alignment at Site H.

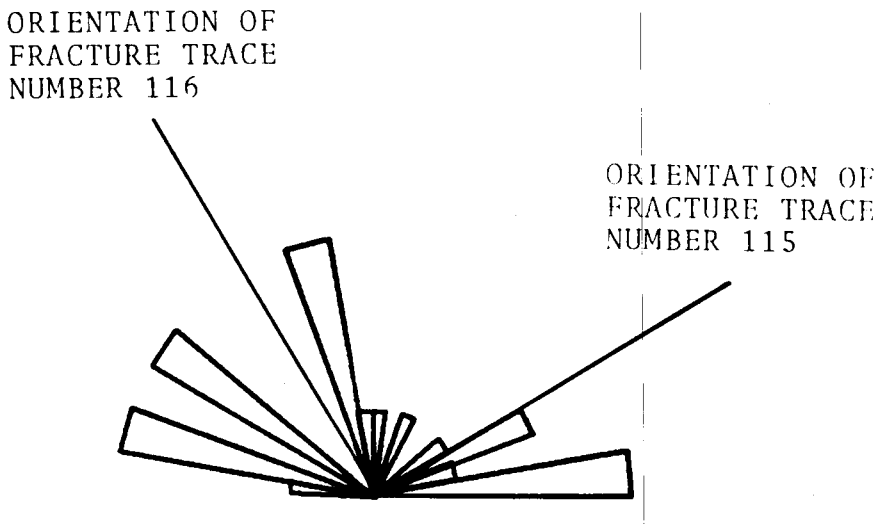


Figure 11. Histogram of bedrock joint orientations for Site H with the orientations of Fracture Trace Numbers 115 and 116 shown. Histogram is based on twenty measurements.

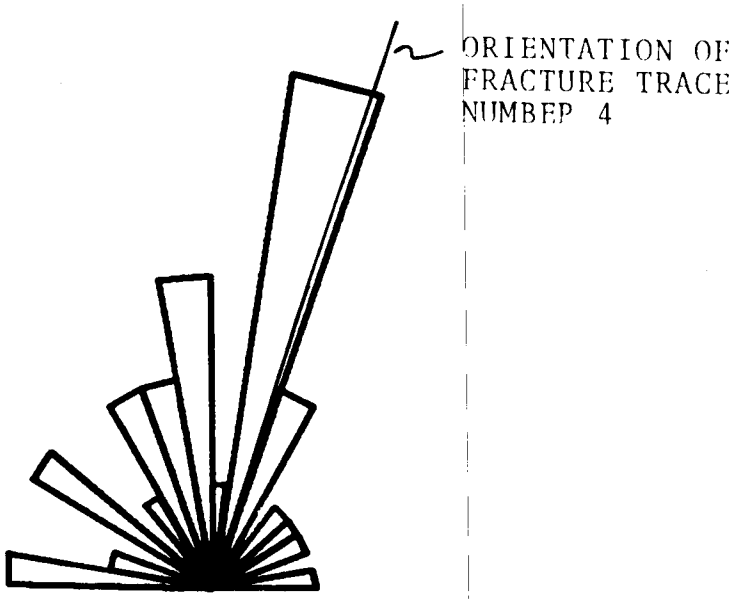


Figure 12. Histogram of bedrock joint orientations for Site C with the orientation of Fracture Trace Number 4 falling within the largest class. The histogram is based on twenty-five measurements.

and a spacing of five feet between each fracture was observed in the silty shale at this site. The photogeologic fracture trace for this site, H109, has an orientation of N325° (Figure 13). H109 is an extremely straight valley alignment.

Site P—Rock Creek, Huntsville Quadrangle

Two outcrops were measured at Site P. The first outcrop was intersected by Fracture Trace #955 which is a straight stream valley. Unfortunately because of the small size of the outcrop only four joint orientations could be measured. More measurements were made at an outcrop about one thousand feet east of the first exposure, but these fractures did not have the same orientations as the photogeologic fracture trace (Figure 14).

Operator Consistency

If the photointerpreter is not consistent in drawing the lineaments and fracture traces, the resulting map will have a change in the linear feature pattern across the map that is not due to changing geology of the area. Since one goal of this study was to define any changes in fracture orientation across the Wartburg Basin, it was important to demonstrate the consistency of this author in photointerpretation of fracture traces and lineaments.

For this purpose, three photographs and their stereopairs were selected across the study area. The photographs were mapped on three separate dates, at least one month apart, to allow time for the

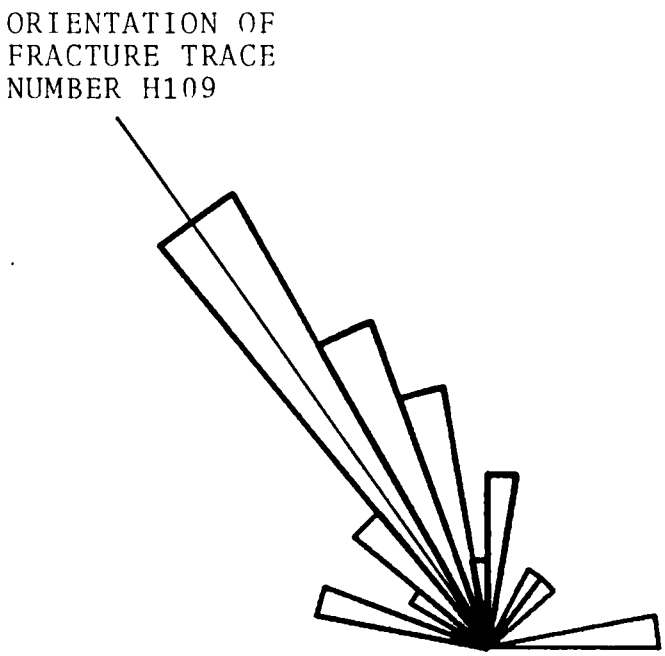


Figure 13. Histogram of bedrock joint orientations for Site F with the orientation of Fracture Trace Number H109 falling within the largest class. The histogram is based on twenty-five measurements.

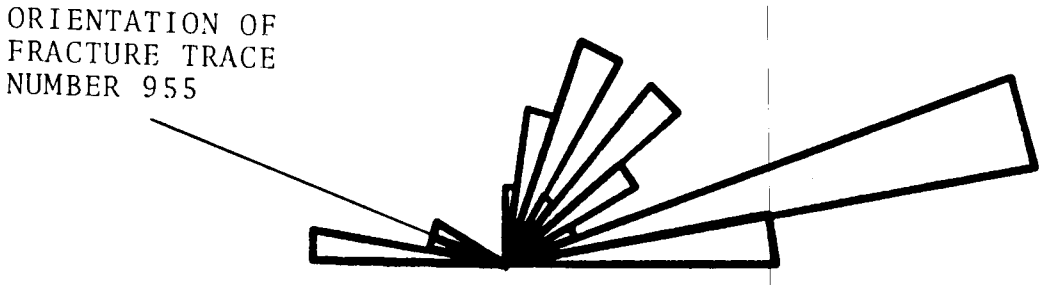


Figure 14. Histogram of bedrock joint orientations for Site P with the orientation of Fracture Trace Number 955 shown. The histogram is based on twenty-eight measurements.

photointerpreter to forget the previously mapped features. The results are shown in Table 4. Only 13% to 21% of the linear features were drawn only once. Thus, 79 to 87% of the linear features were mapped at least twice.

TABLE 4

DEMONSTRATION OF OPERATOR CONSISTENCY BY REPETITIVE DRAWING OF LINEAMENTS AND FRACTURE TRACES ON THREE PHOTOGRAPHS ON THREE SEPARATE DATES

Photo Number	Percentage of Linear Features Drawn only Once	Percentage of Linear Features Drawn Twice	Percentage of Linear Features Drawn all Three Times
155	18	28	54
178	13	23	64
37	21	24	55

CHAPTER VI

ANALYSIS AND INTERPRETATION OF THE PHOTOGEOLOGIC LINEAR FEATURE MAP

Introduction

To interpret a lineament and fracture trace map, statistical analysis is needed to summarize the data on the map. This can be done in a wide variety of ways. Blanchet (1957) used azimuth frequency diagrams and a "fracture-incidence map" showing the number of fractures per unit area. Akimova et al. (1978) prepared charts of selected joint strikes from their main lineament map. Joint density charts were then prepared for the selected strikes. Podwysocki (1974b) analyzed fracture trace lengths and frequency by trend surface analysis. He also analyzed rose diagrams using a multivariate analysis technique which grouped the rose diagrams on the basis of similarity.

For this project, three methods were chosen to analyze the linear feature map. First, to determine the effects of lithology on fracture density, fracture trace density for each geologic formation was calculated. Second, a contour map of fracture frequency was constructed for Ketchen and Jellico West Quadrangles in order to relate the density of fracturing to the structural geology of these areas. Finally, azimuth frequency histograms across the area were drawn in order to summarize the linear feature orientations across the basin.

Effects of Lithology on Photogeologic Fracture Density

Harris et al. (1960) recognized three factors that can influence bedrock fracture density: bedding thickness, lithology and structure within an area. During this study, each of these factors were considered.

For the purposes of this research, bedding thickness is not considered an important factor for several reasons. First, the thicknesses of bedding in all of the formations within the study area were similar, ranging from thin to thick bedded within each of the formations. Secondly, all linear features mapped were much larger than the largest bed within any one formation. In fact, many linear features were mapped over more than one formation (Figure 15). Finally, many of the joints observed in the field cut through several beds. Thus, bedding thickness probably does not greatly affect the density of photogeologic fracturing in the study area.

Likewise, there are several reasons why lithology is probably not an important factor in controlling the density of photogeologic fracturing in this area. First of all, many of the lineaments and fracture traces were mapped across several formations (Figure 15). Secondly, the lithologies of the formations within the study area are similar; each formation consisting of sandstone, siltstone, shale and coal. However, when a clear acetate copy of the linear feature map was laid over a geologic map of Ketchen Quadrangle, fewer linear features seemed to fall within two formations; the Hignite Formation and the Cantron Formation.

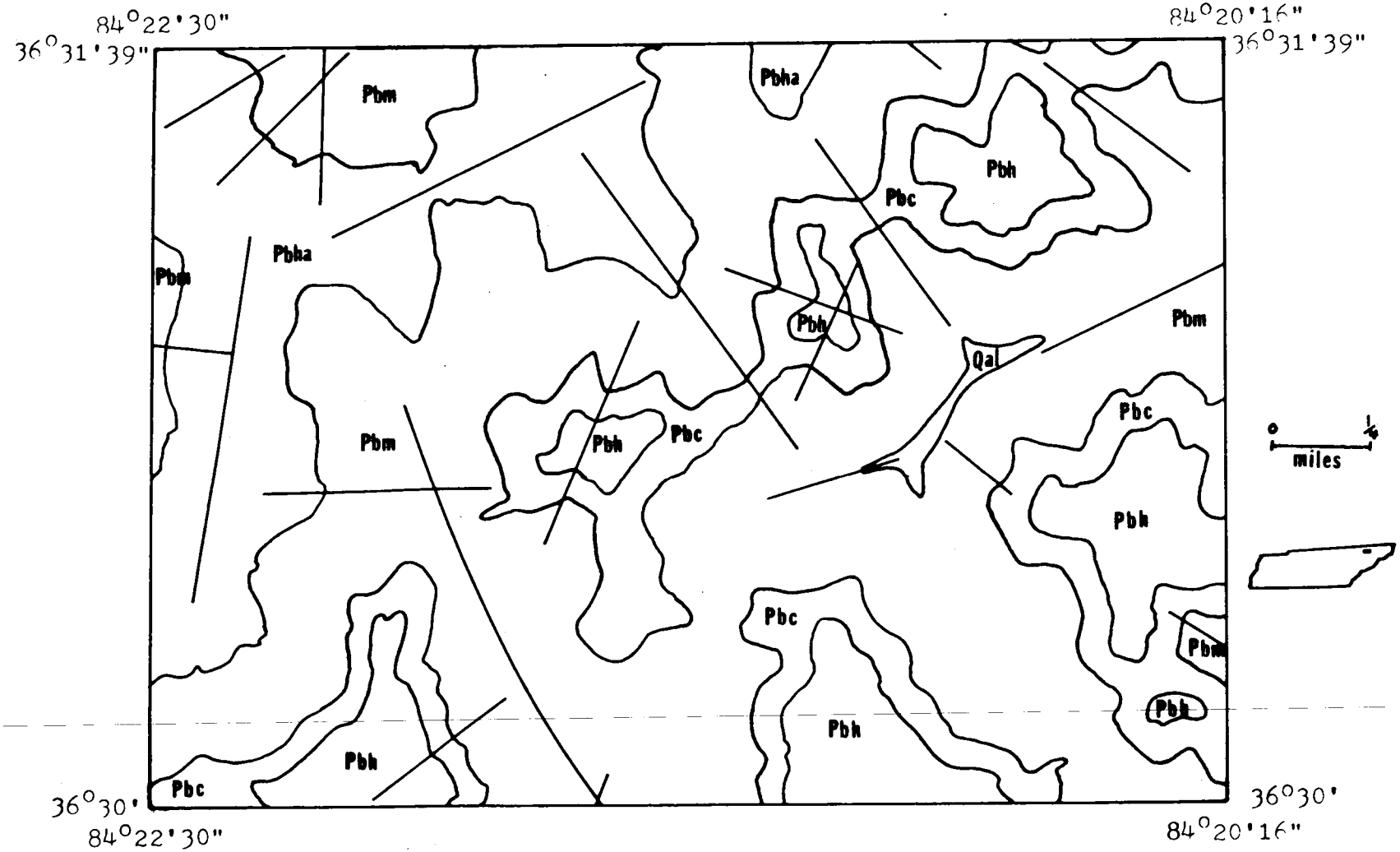


Figure 15. Geologic and fracture trace map of southwest corner of Ketchen Quadrangle. Most of the fracture traces were mapped across more than one formation. Geologic map is by England (1966).

To quantify this observation, a counting grid was laid over the southwest corner of Ketchen Quadrangle which is shown in Figure 15. The number of grid cells falling within each formation was tabulated. The density of fracturing was calculated by dividing the total length of the fractures within a formation by the unit area of that formation. The results are presented in Table 5. From this table, this relationship can be seen: the lower a formation is in the stratigraphic column, the greater the fracture density. This unusual relationship suggests that density calculations have been biased in some way. A possible explanation for this bias is that all formations have an equal fracture density, but erosion has removed the upper formations in the densely fractured areas more rapidly than in areas with less fracturing. Thus, in areas of high fracture density, formations lower in the stratigraphic column would have more areal exposure giving rise to the impression that the lower formations are more densely fractured. The only place one could test this hypothesis would be in an area of steeply dipping beds but no such area occurs in the Wartburg Basin.

Effects of Local Structure on Fracture Density

Since lithology and bedding thickness appear to have little control over the density of lineaments and fracture traces in the study area, it seems logical that the structural geology of the area does. To test this idea, contour maps of lineament and fracture trace frequency were drawn for the Ketchen and Jellico West Quadrangles (these are the only two quadrangles in the study area which have geologic maps at a scale of

TABLE 5

A COMPARISON OF FRACTURE DENSITY FOR FOUR FORMATIONS IN KETCHEN QUADRANGLE

Formation Name	Fracture Density
Hignite Formation (Pbh)	.0031
Catron Formation (Pbc)	.0039
Mingo Formation (Pbm)	.0077
Hance Formation (Pbha)	.0134

Formations are listed in order with the stratigraphically top unit at the top of the table. (Data are taken from the map shown in Figure 15).

1:24,000). At the beginning, contour maps of both fracture frequency (number of fractures per unit area) and fracture density (total fracture length per unit area) were drawn. Since they were found to be almost exactly alike, fracture frequency was used because it was easier to calculate.

The following procedure was used to construct the fracture frequency maps. A grid was laid over the lineament and fracture trace map and a counting square was moved along the grid. After several tries, a counting square of .66 by .66 miles was found to work best. As the counting square was moved along the grid, the number of linear features within the square were recorded in the center of the square. The distance between each recorded number was .33 miles. This procedure produced a grid of numbers which was then contoured at the intervals of five, seven and nine fractures per .44 square miles.

The resulting fracture frequency contour maps (Figures 16 and 17) were combined with structural contour maps from Ketchen and Jellico West (from Englund, 1966 and Englund, 1969). It can be seen from these maps that the local structure of the area does influence the photogeologic fracture frequency. Fracture frequency increases on the limbs of folds and reaches a maximum on the noses of folds. The areas with the highest density of fractures are those with the maximum amount of folding. There is one exception to this rule, in the eastern portion of the Jellico West Quadrangle, where fracture density is very low and yet there is a great amount of folding. However, this can be explained by reference to the geologic map of Jellico West. The

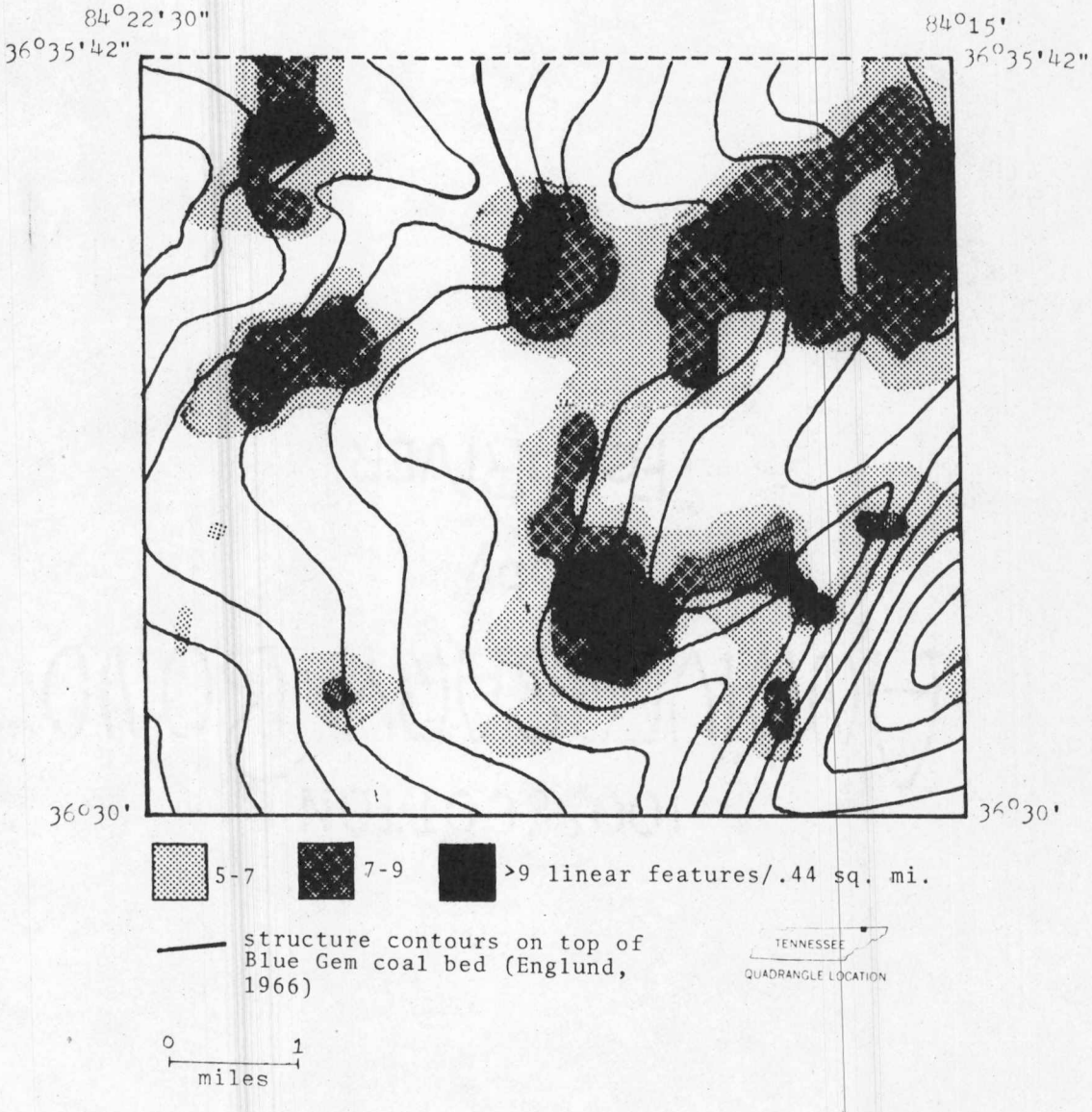


Figure 16. Fracture frequency map superimposed on a structure contour map of Ketchen Quadrangle.

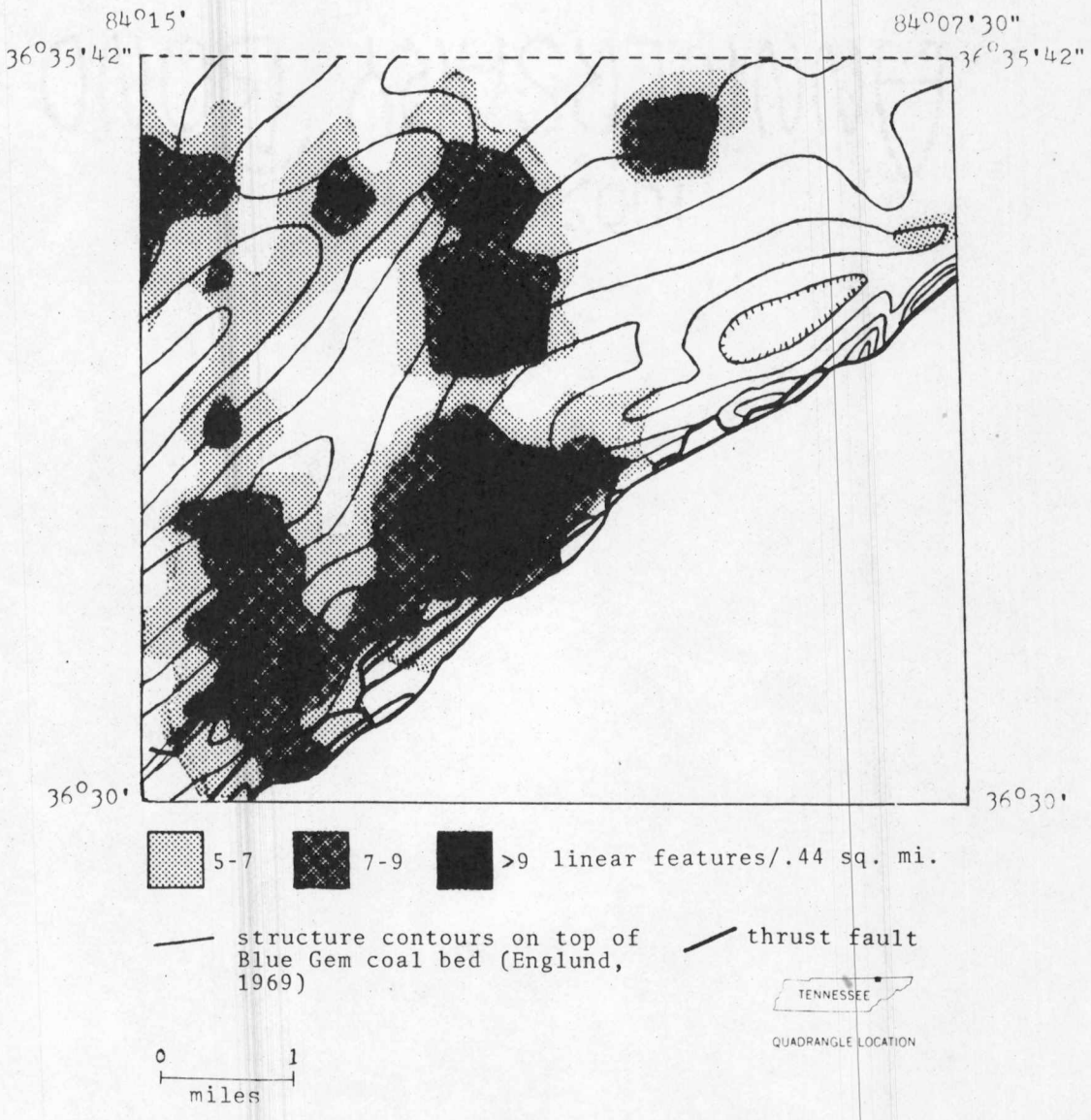


Figure 17. Fracture frequency map superimposed on a structure contour map of Jellico West Quadrangle.

eastern portion of that quadrangle has a large amount of land covered by alluvium, towns, and strip mined areas. Alluvium masks the lineament and fracture traces and strip mining and towns destroy all traces of fracturing (Parizek, 1971).

Lineament and Fracture Trace Orientations Across the Wartburg Basin

A computer program written by Podwysocki (1974a) was used to summarize the lineament and fracture trace orientations across the Wartburg Basin (Figure 18). The program uses the digitized end points of linear features to calculate their azimuths. The program divides the study area into a grid of cells of user specified dimensions. Lineaments in each grid cell are placed into 10° classes based on their orientations and a rose diagram which summarizes the lineament frequency data is plotted for each grid cell.

From the orientations of the rose diagrams in Figure 18, tentative conclusions may be drawn. It appears that the jointing in the study area originates from both tension and shear stress because for most of the histograms there are more than two prominent directions of fracturing. Some of the roses even approximate the idealized joint distribution normally associated with anticlines (Figure 19). Local variations in the orientation of folding might have caused the wide blades and the extra blades of some of the roses.

Because the fracture frequency in Jellico West and Ketchen Quadrangle is related to the local folding, the fold axes can be used to interpret the rose diagrams for these quadrangles. The maximum

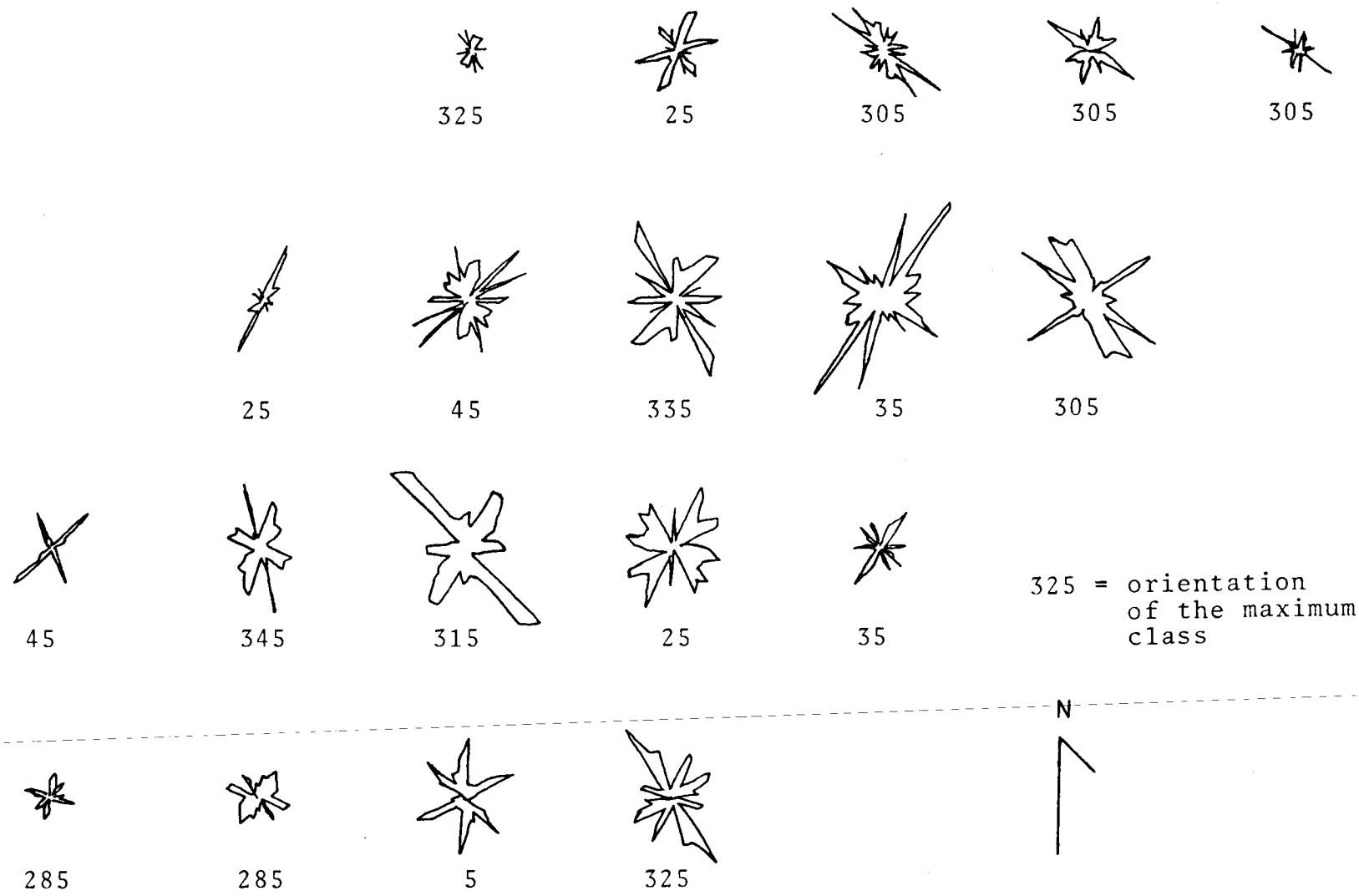


Figure 18. Rose diagrams for lineaments and fracture traces across the Wartburg Basin.

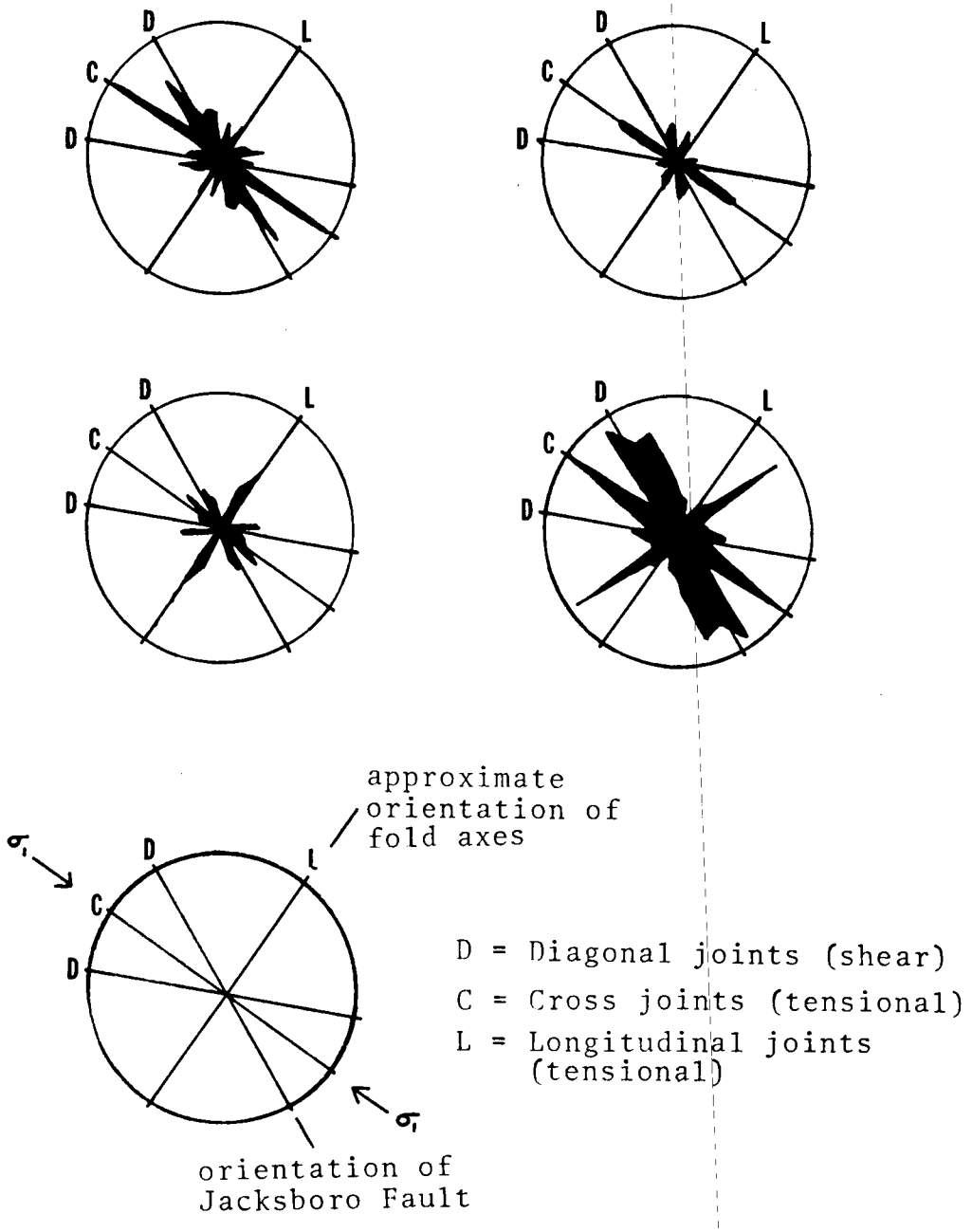


Figure 19. A comparison of the rose diagrams from the eastern side of the Wartburg Basin to the idealized joint distribution associated with folding. The stereogram of idealized joint distribution (Badgely, 1965 and Price, 1966) was oriented using local fold axes and the orientation of the Jacksboro Fault as references.

class for each of the rose diagrams was measured. For Jellico West and the eastern half of Pioneer and Ketchen Quadrangles, the maximum class of the roses was either N350° or N35°. These orientations are perpendicular to each other. The strike of the fold axes in Jellico West and Ketchen is approximately between N35° and N50°. Therefore, the joint set which is oriented at N35° would be classified as longitudinal joints and those at N305° would be cross joints (Badgley, 1965). Both of these joint types are tension joints. The Jacksboro Fault which is a strike slip fault, is oriented 25° away from the orientation of the cross joints. Since the typical angle between shear and extension fractures is approximately 30° (Badgley, 1965), this is further evidence that the joints oriented at N305° are cross joints. Using this logic, several rose diagrams from the eastern side of the study area are related to the idealized joint distribution associated with folds in Figure 19.

None of the other rose diagrams, except for those on the eastern side of the map, have a maximum of N35° or N305°. This might be related to the change in folding that occurs approximately in the center of Ketchen Quadrangle. To the east of this line, folds are regular and fold axes are oriented to the northeast. On the west, the folding becomes extremely shallow and the orientations of the fold axes become irregular. How the local structure influences the jointing to the west of Ketchen is unknown at this time since there are no large scale geologic maps for this area.

CHAPTER VII

CONCLUSIONS

Three types of photogeologic linear features were mapped on the aerial photography: alignments of vegetation, topographic-erosional alignments and soil tone alignments. Most of the linear features mapped were of topographic-erosional expression. These consisted of alignments of straight stream segments or valley axes. Soil fracture traces were actually a combination of two factors: dark soil and dark green, lush vegetation which could be due to increased soil moisture over zones of bedrock fractures. Vegetation fracture traces were of two types: alignments of higher standing trees and alignments of darker Hemlock trees in a deciduous forest. Since Hemlock trees grow in moist soils, this alignment of vegetation could be due to groundwater seepage associated with a zone of bedrock fractures. An alignment of higher standing trees could be healthier vegetation also growing over an area of increased soil moisture.

Orientations of lineaments and fracture traces in most cases reflected the orientations of bedrock joints measured in the field. Histograms of strike frequencies of bedrock joints were usually similar to histograms of photogeologic linear feature orientations that fell within one to 1.5 miles (1.6 to 2.4 kilometers) of the field site. Dissimilar histograms might be a result of insufficient bedrock joint measurements at small outcrops or low photogeologic linear feature density for that area. In most cases, where bedrock exposures

were intersected by a fracture trace, the orientation of the fracture trace fell within the largest joint orientation class.

The lithologies of the formations in the research area seem to have little or no control over the photogeologic fracture density. However the local structural geology of the area does have a definite effect on the fracture density pattern. Fracture frequency, which is similar to fracture density, increases on the flanks and noses of folds where the maximum amount of folding has occurred. Fracture frequency maps could be used to locate oil bearing structures such as domes or anticlines. For this area, the fracture frequency patterns associated with these structures are closed rings or u-shaped patterns because in the study area, fracture frequency increases on the flanks of folds.

Fracture frequency decreases in areas covered by alluvium, strip mined areas, and areas covered by towns. Obviously, in lineament and fracture trace studies, the earliest photographs available would be useful to avoid information lost to strip mines and cities.

Based on a study of the photogeologic linear feature orientations in the study area, both shear fractures and tension fractures are probably present. In the eastern part of the study area, the maximum class of fracture orientations are due to tension stress. A change in the orientation of the maximum class occurs in the middle of Ketchen Quadrangle where the folds flatten out and become irregular in orientation. Thus, fracture traces and lineament orientation studies can be used to locate changes in the structure of the

Wartburg Basin. However, the cause of these changes are not apparent without additional information on the local structural geology of the area.

LIST OF REFERENCES

LIST OF REFERENCES

Akimova, Y. V., Berlyant, A. M. and Volchanskaya, I. K., 1978, Analysis of structural jointing from cartographic and aerospace materials: International Geologic Review, v. 20, no. 5, pp. 569-574.

Allum, J. A., 1966, Photogeology and regional mapping: Pergamon Press, New York, 107 p.

Alpay, O. A., 1973, Application of aerial photographic interpretation to the study of reservoir natural fracture systems: Journal Petroleum Technology, v. 25, no. 1, pp. 37-45.

Avery, T. E., 1962, Interpretation of aerial photographs: Burgess Publishing Company, Minneapolis, 192 p.

Badgely, P. C., 1965, Structural and tectonic principles: Harper and Row, New York, 521 p.

Barlow, J. A., 1969, Stratigraphy and paleobotany of the youngest Pennsylvania strata in the Caryville, Tennessee area: Unpublished doctoral dissertation, The University of Tennessee, Knoxville.

Billings, M. P., 1962, Structural geology: Prentice-Hall, Inc., Englewood Cliffs, New Jersey, 606 p.

Blanchet, P. D., 1957, Development of fracture analysis as exploration method: Bulletin of American Association of Petroleum Geologists, v. 41, no. 8, pp. 1748-1759.

Boyer, R. E. and McQueen, J. E., 1964, Comparison of mapped rock fractures and airphoto linears: Photogrammetric Engineering, v. 30, no. 4, pp. 630-635.

Brown, C. W., 1961, Comparison of joints, faults and airphoto linears: Bulletin of American Association of Petroleum Geologists, v. 45, no. 11, pp. 1888-1892.

Burns, K. L. and Brown, G. H., 1978, The human perception of geological lineaments and other discrete features in remote sensing imagery: Remote Sensing of the Environment, v. 7, no. 2, pp. 163-176.

Chayes, F., 1949, Statistical analysis of two dimensional fabric diagrams, in Fairbairn, W. H., ed., Structural petrology of deformed rocks: Addison-Wesley Press, Cambridge, Mass., 344 p.

Desitter, L. U., 1964, Structural Geology: McGraw-Hill, New York, 587 p.

Englund, K. J., 1966, Geologic map of the Ketchen Quadrangle, Tennessee-Kentucky: U.S. Geological Survey Quadrangle Map GQ-500.

Englund, K. J., 1969, Geologic map of the Jellico West Quadrangle, Kentucky-Tennessee: U.S. Geological Survey Quadrangle Map GQ-855.

Gillerman, E., 1970, Roselle lineament of Southeast Missouri: Geological Society of America Bulletin, v. 81, pp. 975-982.

Gol'braikh, I. C., Zabaluyev, V. V., Lastochkin, A. N., Mirkin, G. R. and Reinin, I. V., 1968, Morphostructural methods for the tectonic study of covered platform oil and gas regions: NEDRA Publishing House, Leningrad, 137 p.

Gold, D. P., Parizek, R. R. and Alexander, S. A., 1973, Analysis and application of ERTS-1 data for regional geological mapping: in Symposium on significant results obtained from the Earth Resources Technology Satellite-1, v. I, NASA, Washington, D.C., pp. 231-239.

Gwinn, V. E., 1964, Thin-skinned tectonics in the plateau and northwestern Valley and Ridge provinces of the Central Appalachians: Geological Society of America Bulletin, v. 75, pp. 863-899.

Halbouty, M. T., 1976, Application of LANDSAT imagery to petroleum and mineral exploration: Bulletin of American Association of Petroleum Geologists, v. 60, no. 5, pp. 745-793.

Haman, P. J., 1961, Lineament analysis on aerial photographs: West Canadian Research Publications of Geology and Related Sciences, series 2, no. 1, 23 p.

Haman, P. J., 1964, Geomechanics applied to fracture analysis on aerial photographs: West Canadian Research Publications of Geology and Related Sciences, series 2, no. 2, 84 p.

Harris, J. F., Taylor, G. L. and Walper, J. L., 1960, Relation of deformational fractures in sedimentary rocks to regional and local structures: Bulletin of American Association of Petroleum Geologists, v. 44, no. 12, p. 1853.

Harris, L. D. and Milici, R. C., 1977, Characteristics of thin-skinned style of deformation in the Southern Appalachians and potential hydrocarbon traps: U.S. Geological Survey Professional Paper 1018, 40 p.

Hobbs, B. E., Means, W. D. and Williams, P. F., 1976, An outline of structural geology: John Wiley and Sons, Inc., New York, 554 p.

Hobbs, W. H., 1904, Lineaments of the Atlantic Border Region: Geological Society of America Bulletin, v. 15, pp. 483-506.

Hobbs, W. H., 1911, Repeating patterns in the structure of the land: Geological Society of America Bulletin, v. 22, pp. 123-176.

Hodgson, R. A., 1961, Classification of structures on joint surfaces: American Journal of Science, v. 259, pp. 493-502.

Holz, R. K., ed., 1973, The surveillant science-remote sensing of the environment: Houghton Mifflin Company, Boston, 309 p.

Horton, R. A., 1977, Structural analysis of the Jacksboro Fault, East Tennessee: Unpublished masters thesis, The University of Tennessee, Knoxville.

Huntington, J. F. and Raiche, A. P., 1978, A multi-attribute method for comparing geological lineament interpretations. Remote Sensing of the Environment, v. 7, no. 2, pp. 145-161.

Kaiser, E. P., 1950, Structural significance of lineaments: (abs.) Geological Society of America Bulletin, v. 61, no. 12, pp. 1475-1476.

Komar, C. A., Overbey, W. K. Jr., Rough, R. L. and Lambert, W. G., 1971, Factors that predict fracture orientation in a gas storage reservoir: Journal of Petroleum Technology, v. 23, no. 5, pp. 546-550.

Lahee, F. H., 1961, Field geology: McGraw-Hill Book Comapny, New York, 926 p.

Lattman, L. H., 1958, Technique of mapping geologic fracture traces and lineaments on aerial photographs: Photogrammetric Engineering, v. 24, no. 4, pp. 568-576.

Lattman, L. H. and Matzke, R. H., 1961, Geologic significance of fracture traces: Photogrammetric Engineering, v. 27, no. 3, pp. 435-438.

Lattman, L. H. and Nickelson, R. P., 1958, Photogeologic fracture trace mapping in the Appalachian Plateau: Bulletin of the American Association of Petroleum Geologists, v. 42, no. 9, pp. 2238-2245.

Lattman, L. H. and Ray, R. G., 1965, Aerial photographs in field geology: Holt, Rinehart and Winston, New York, 221 p.

Luther, E. T., 1959, The coal reserves of Tennessee: Tennessee Division of Geology, Bulletin 63, 294 p.

Miller, V. C. and Miller, C. F., 1961, Photogeology: McGraw-Hill, New York, 248 p.

Moore, G. K. and Hollyday, E. F., 1976, Discovery of the Beach Grove Lineament of Tennessee, in A new window on our planet: U.S. Geological Survey Professional Paper 929, pp. 164-168.

Moore, J. D., Moravec, G. F. and Hinkle, F., 1975, The relationship between lineaments and ground-water hydrology using ERTS images: Geological Society of America, Abstracts, v. 7, no. 4, p. 519.

Nickelson, R. P. and Hough, V. D., 1967, Jointing in the Appalachian Plateau of Pennsylvania: Geological Society of America Bulletin, v. 78, pt. 1, pp. 609-629.

Ollier, C. D., 1977, Terrain classification—methods, applications and principles: in Hails, J. R. (ed.), Applied geomorphology, Elsevier Scientific Publishing Company, New York. pp. 277-316.

Overby, W. K., Jr., and Rough, R. L., 1968, Surface-joint patterns predict well-bore fracture orientation: Oil and Gas Journal, v. 66, no. 9, pp. 84-86.

Parizek, R. R., 1971, Impact of highways on the hydrogeologic environment: in Environmental geomorphology, New York State University, Binghamton, New York, pp. 151-199.

Parker, J. M. III, 1942, Regional systematic jointing in slightly deformed sedimentary rocks: Geological Society of America Bulletin, v. 53, pp. 381-408.

Parry, J. T. and Turner, H., 1971, Infrared photos for drainage analysis: Photogrammetric Engineering, v. 37, pp. 1031-1038.

Petrides, G. A., 1972, A field guide to trees and shrubs: Houghton Mifflin Company, Boston, 428 p.

Podwysocki, M. H., 1974a, FORTRAN IV programs for summarization and analysis of fracture trace and lineament patterns: NASA Goddard Space Flight Center Document X-923-74-200, 88 p.

Podwysocki, M. H., 1974b, An analysis of fracture trace patterns in areas of flat-lying sedimentary rocks for detection of buried geologic structure: NASA Goddard Space Flight Center Document X-923-74-222, 37 p.

Podwysocki, M. H., Moik, J. G. and Shoup, W. C., 1975, Quantification of geologic lineaments by manual and machine processing techniques: NASA Goddard Space Flight Center Document X-923-75-183, 23 p.

Price, N. J., 1966, Fault and joint development in brittle and semi-brittle rock: Pergamon Press, New York, 176 p.

Ray, R. G., 1960, Aerial photographs in geologic interpretation and mapping: U.S. Geologic Survey Professional Paper 373, 227 p.

Roberts, J. C., 1961, Feather-fracture and the mechanics of rock-jointing: American Journal of Science, v. 259, pp. 481-492.

Roberts, T. A., 1978, Transitional lower delta plain-upper delta plain sediments in Middle Pennsylvanian coal-bearing strata Eastern Wartburg Basin, Tennessee: Unpublished masters thesis, The University of Tennessee, Knoxville.

Rodgers, J., 1970, The tectonics of the Appalachians: Wiley-Interscience, New York, 271 p.

Sabins, F. F. Jr., 1978, Remote sensing—principles and interpretation: W. H. Freeman and Company, San Francisco, 425 p.

Slusarski, M., 1979, Photogeologic fracture traces and lineaments in the Wartburg Basin Section of the Cumberland Plateau Physiographic Subprovince, Tennessee: Unpublished masters thesis, The University of Tennessee, Knoxville.

Spencer, E. W., 1969, Introduction to the structure of the earth: McGraw-Hill Book Company, New York, 597 p.

Tisdale, R. M., 1974, Field characteristics and recognition of upper delta plain sediments, Vowell Mountain and Cross Mountain Formations, Windrock Quadrangle, Tennessee: Unpublished masters thesis, The University of Tennessee, Knoxville, 128 p.

Trainer, F. W., 1967, Measurement of the abundance of fracture traces on aerial photographs: U.S. Geological Survey Professional Paper 575-C, pp. C184-C188.

Van Lopik, J. R. and Kolb, C. R., 1959, A technique for preparing desert terrain analogs: U.S. Army Engineer Waterways Experiment Station Technical Report No. 3-506, Vicksburg, Mississippi, 70 p.

Wilson, C. W., Jewell, J. W. and Luther, E. T., 1956, Pennsylvanian geology of the Cumberland Plateau: Tennessee Division of Geology, Folio, 21 p.

Wilson, C. W. and Stearns, R. G., 1958, Structure of the Cumberland Plateau, Tennessee: Geological Society of America Bulletin, v. 69, pp. 1283-1296.

Wobber, F. J., 1967, Fracture traces in Illinois: Photogrammetric Engineering, v. 33, pp. 499-506.

APPENDICES

APPENDIX A

COMPUTER PROGRAM TO DRAW ROSE DIAGRAMS

```
C  PROGRAM TO READ ENDPOINTS OR AZIMUTHS OF LINES AND DRAW
C  A ROSE DIAGRAM FOR THE LINES

      INTEGER PTR, IX, IY, IX2, IY2, I, LUN
      REAL AZM, Q(18), R(18), CLASS(18), X, Y
      REAL X2, Y2

      DATA CLASS/18*0.0/
      DATA Q/20.,40.,60.,80.,100.,120.,140.,
     9160.,180.,200.,220.,240.,260.,280.,300.,320.,340.,
     9360./
      DATA R/0.,20.,40.,60.,80.,100.,120.,140.,
     9160.,180.,200.,220.,240.,260.,280.,300.,320.,340./

C  USER SPECIFIES TYPE OF INPUT DATA, ENDPOINTS OR AZIMUTH
      WRITE(5,10)
 10   FORMAT(' TYPE 20 FOR ENDPOINTS, 21 FOR AZIMUTHS ')
      READ(5,15) LUN
 15   FORMAT(I3)
      IF (LUN.EQ.20) GO TO 25
C  LOOP TO READ AZIMUTH FILE AND PUT AZIMUTHS IN 10
C  DEGREE CLASSES
      DO 20 I=1,1000
      READ (LUN,17) DATA
 17   FORMAT (F15.9)
```

```
      IF (DATA.EQ.-99.) GO TO 150
      AZM=DATA
C  CHANGE 0-360 BRUNTON READINGS TO AZIMUTHS ACCEPTABLE
C  TO PROGRAM
      IF (DATA.LE.90) AZM=DATA*(-1)+90
      IF (DATA.GT.270.AND.DATA.LE.360) AZM=360-DATA+90
      IF (DATA.GT.90.AND.DATA.LE.270) AZM=180-DATA+90
      WRITE (22,18) AZM
18    FORMAT (F15.9)
      IF (AZM.EQ.180..OR.AZM.EQ.0.) CLASS(1)=CLASS(1)+.5
      IF (AZM.EQ.180..OR.AZM.EQ.0.) CLASS(18)=CLASS(18)+.5
      IF (AZM.EQ.180..OR.AZM.EQ.0.) GO TO 20
      PTR=AZM/10.+1.
      CLASS(PTR)=CLASS(PTR)+1
20    CONTINUE

C  LOOP TO READ ENDPOINTS AND CALCULATE AZIMUTH

25    DO 100 I=1,200
      READ (20,50) IX,IY,IX2,IY2
50    FORMAT (2I10)

C  -99 SIGNALS THE END OF DATA
      IF (IX.EQ.-99) GO TO 150
```

```
C   IN CASE OF A DUE EAST AZIMUTH
          IF (IY.EQ.IY2) CLASS(1)=CLASS(1)+.5
          IF (IY.EQ.IY2) CLASS(18)=CLASS(18)+.5
          IF (IY.EQ.IY2) GO TO 25

C   IN CASE OF A DUE NORTH AZIMUTH
          IF (IX.EQ.IX2) CLASS(9)=CLASS(9)+1.0
          IF (IX.EQ.IX2) GO TO 25

C   CALCULATE AZIMUTH

          X=IX
          Y=IY
          X2=IX2
          Y2=IY2
          AZM = ATAN2(ABS(Y-Y2),ABS(X-X2))
          AZM = AZM*180/3.1416
          WRITE (22,70) AZM
 70       FORMAT (F15.9)
          IF((X.GT.X2.AND.Y.GT.Y2).OR.(X2.GT.X.AND.Y2.GT.Y))
     1    AZM=AZM*-1.+180.

C   WRITE AZIMUTH TO FOR22.DAT
          WRITE (22,75) AZM
 75       FORMAT(F15.9)
```

```
C  PUT AZIMUTH IN 10 DEGREE CLASSES
        PTR=AZM/10.+1.
 100    CLASS(PTR)=CLASS(PTR)+1
 150    CONTINUE
        WRITE (5,165)
 165    FORMAT (' TYPE SCALING FACTOR LESS THAN 600 ')
        READ (5,175) ISCALE
 175    FORMAT (I3)

C  DRAW ROSE

        CALL INITT(30)
        WRITE (5,185)
 185    FORMAT (' HIT CARRIAGE RETURN FOR ROSE DIAGRAM ')
        CALL TINPUT(ICHAR)

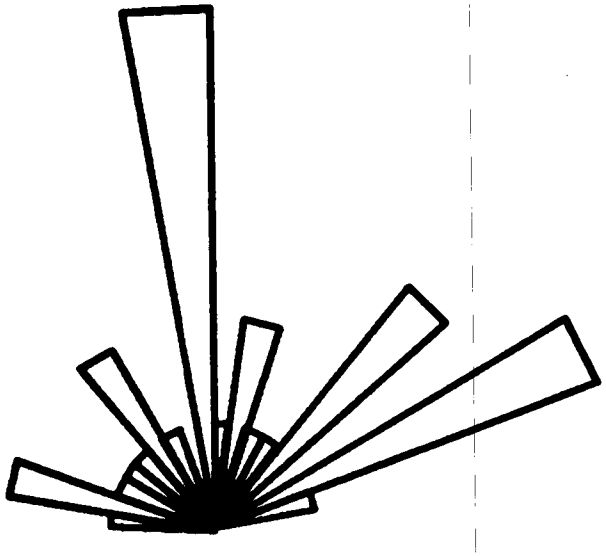
        CALL ERASE
        CALL DWINDO(0.,1000.,0.,360.)
        CALL POLTRN(0.,180.,0.)
        CALL MOVEA(0.,360.)
        DO 200 I=1,18
        CLASS(I)=CLASS(I)*ISCALE
        CALL DRAWA (CLASS(I),Q(I))
        CALL DRAWA (CLASS(I),R(I))
```

```
200     CALL DRAWA(0.,R(I))
        CALL TINPUT
        WRITE (5,225)
225     FORMAT (' HIT C TO INCREASE SCALE AND REDRAW ROSE ')
        CALL TINPUT(ICHAR)
        IF  (ICHAR.EQ.67) GO TO 150
        CALL FINITT(0,760)
        STOP
        END
```

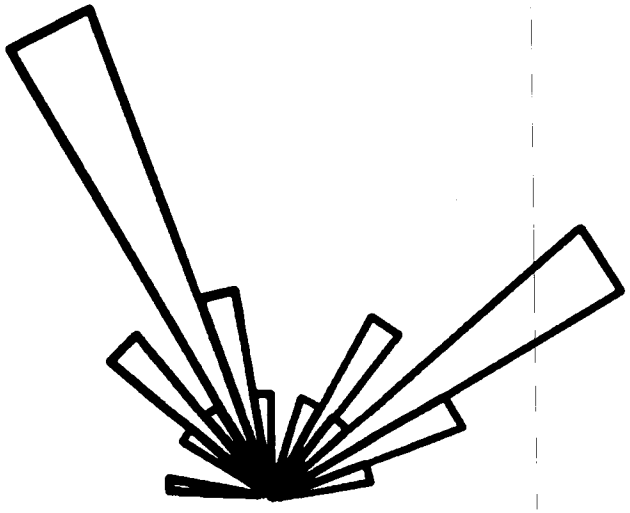
APPENDIX B

HISTOGRAMS OF PHOTOGEOLOGIC LINEAR FEATURES AND BEDROCK JOINTS

SITE A



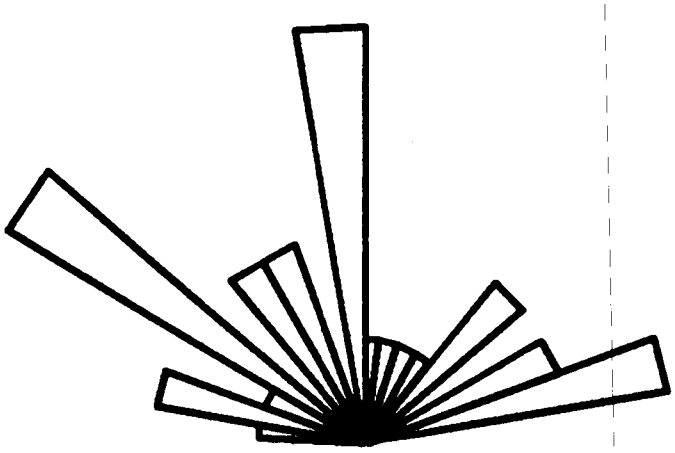
PHOTOGEOLOGIC LINEAR FEATURES



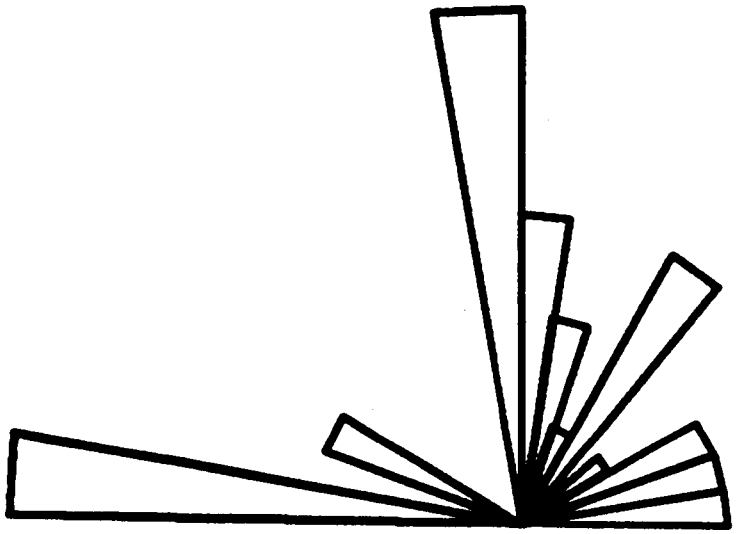
BEDROCK JOINTS

Figure B-1. Histogram of photogeologic linear feature orientations which lie within one mile of site A and histogram of joint orientations from field site A. North is at the top of the page. The top histogram is based on twenty-seven measurements and the bottom histogram is based on twenty-four.

SITE B



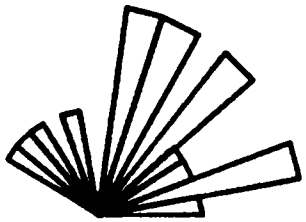
PHOTOGEOLOGIC LINEAR FEATURES



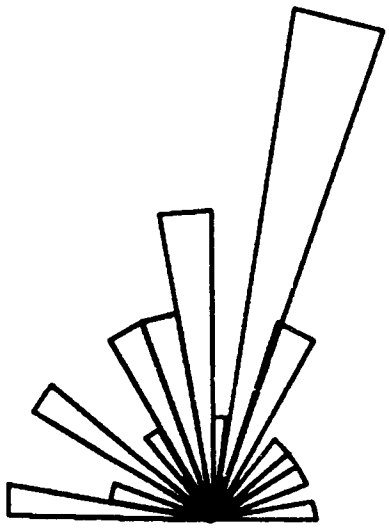
BEDROCK JOINTS

Figure B-2. Histogram of photogeologic linear feature orientations which lie within one mile of site B and histogram of joint orientations from field site B. North is at the top of the page. The top histogram is based on twenty-seven measurements and the bottom is based on twenty-eight.

SITE C



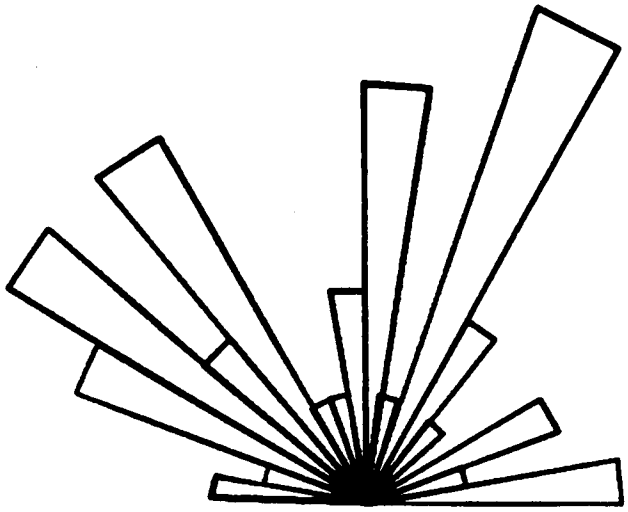
PHOTOGEOLOGIC LINEAR FEATURES



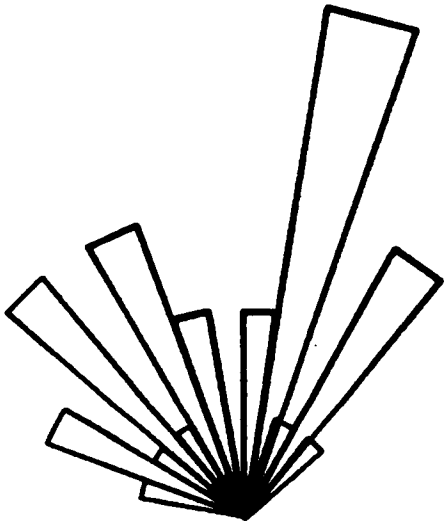
BEDROCK JOINTS

Figure B-3. Histogram of photogeologic linear feature orientations which lie within one mile of site C and histogram of joint orientations from field site C. North is at the top of the page. The top histogram is based on fifteen measurements and the bottom is based on twenty-five.

SITE D



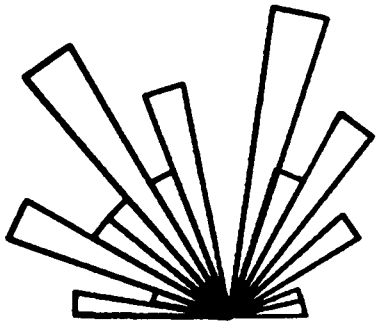
PHOTOGEOLOGIC LINEAR FEATURES



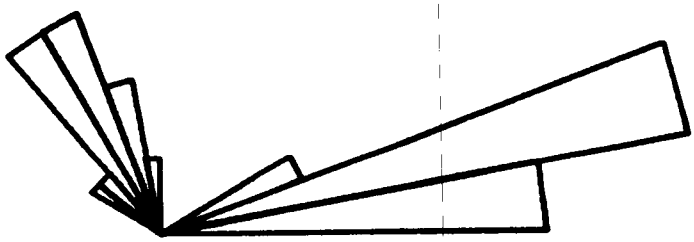
BEDROCK JOINTS

Figure B-4. Histogram of photogeologic linear feature orientations which lie within 1.5 miles of site D and histogram of joint orientations from field site D. North is at the top of the page. The top histogram is based on thirty-four measurements and the bottom is based on twenty-five.

SITE E



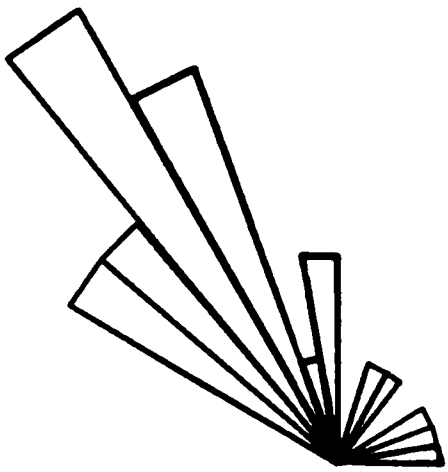
PHOTOGEOLOGIC LINEAR FEATURES



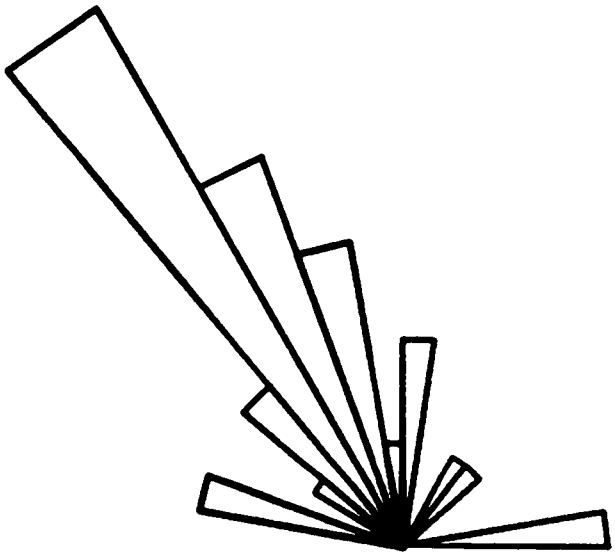
BEDROCK JOINTS

Figure B-5. Histogram of photogeologic linear feature orientations which lie within 1.25 miles of site E and histogram of joint orientations from field site E. North is at the top of the page. The top histogram is based on thirty-two measurements and the bottom is based on twenty-five.

SITE F



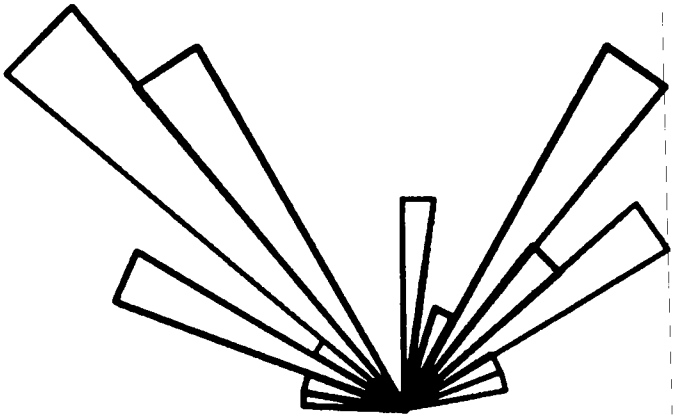
PHOTOGEOLOGIC LINEAR FEATURES



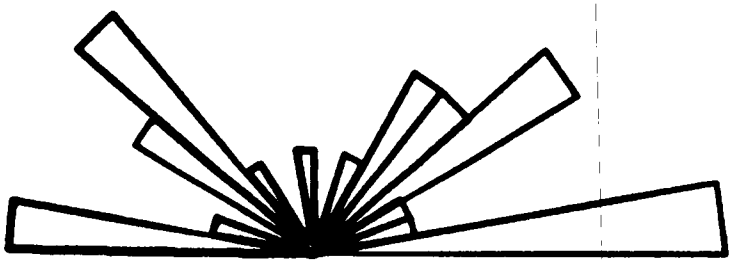
BEDROCK JOINTS

Figure B-6. Histogram of photogeologic linear feature orientations which lie within one mile of site F and histogram of joint orientations from field site F. North is at the top of the page. The top histogram is based on twenty-three measurements and the bottom is based on twenty-five.

SITE G



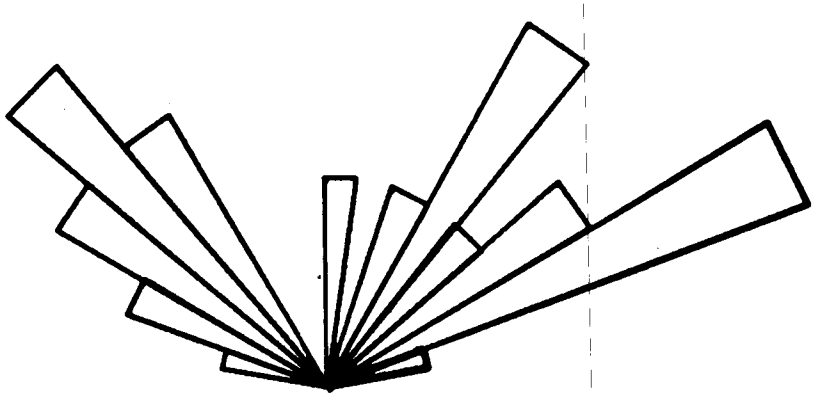
PHOTOGEOLOGIC LINEAR FEATURES



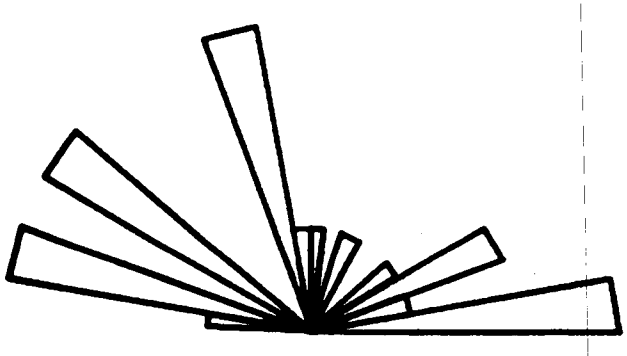
BEDROCK JOINTS

Figure B-7. Histogram of photogeologic linear feature orientations which lie within one mile of site G and histogram of joint orientations from field site G. North is at the top of the page. The top histogram is based on twenty-nine measurements and the bottom is based on twenty-five.

SITE H



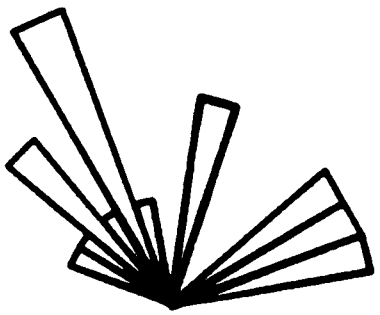
PHOTOGEOLOGIC LINEAR FEATURES



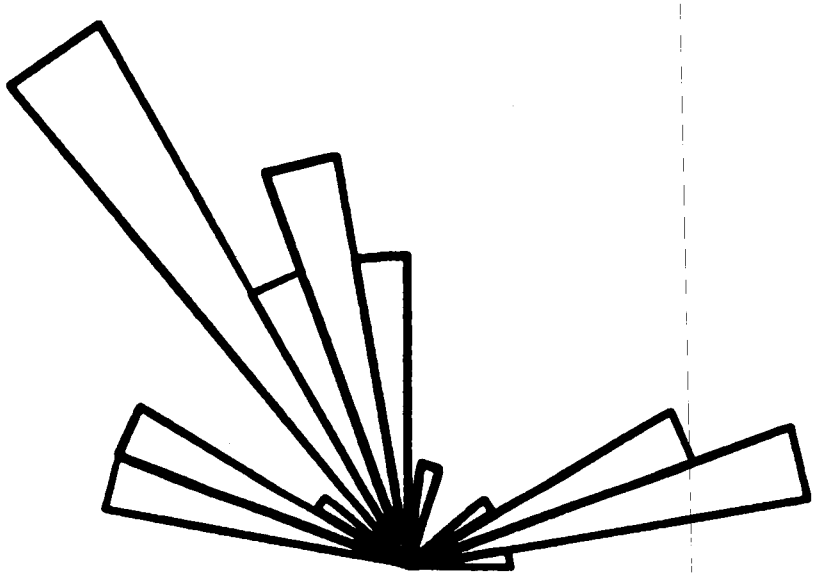
BEDROCK JOINTS

Figure B-8. Histogram of photogeologic linear feature orientations which lie within one mile of site H and histogram of joint orientations from field site H. North is at the top of the page. The top histogram is based on thirty-two measurements and the bottom is based on twenty.

SITE I



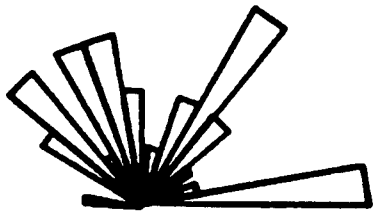
PHOTOGEOLOGIC LINEAR FEATURES



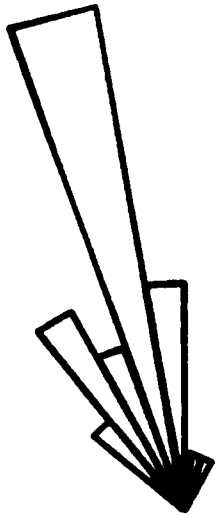
BEDROCK JOINTS

Figure B-9. Histogram of photogeologic linear feature orientations which lie within one mile of site I and histogram of joint orientations from field site I. North is at the top of the page. The top histogram is based on seventeen measurements and the bottom is based on thirty-three.

SITE J



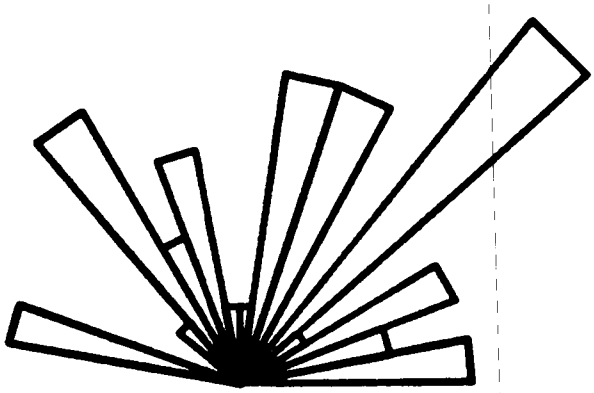
PHOTOGEOLOGIC LINEAR FEATURES



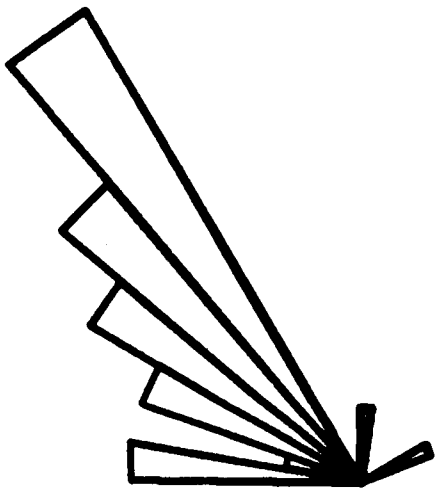
BEDROCK JOINTS

Figure B-10. Histogram of photogeologic linear feature orientations which lie within 1.25 miles of site J and histogram of joint orientations from field site J. North is at the top of the page. The top histogram is based on thirty-one measurements and the bottom is based on twenty-five.

SITE K



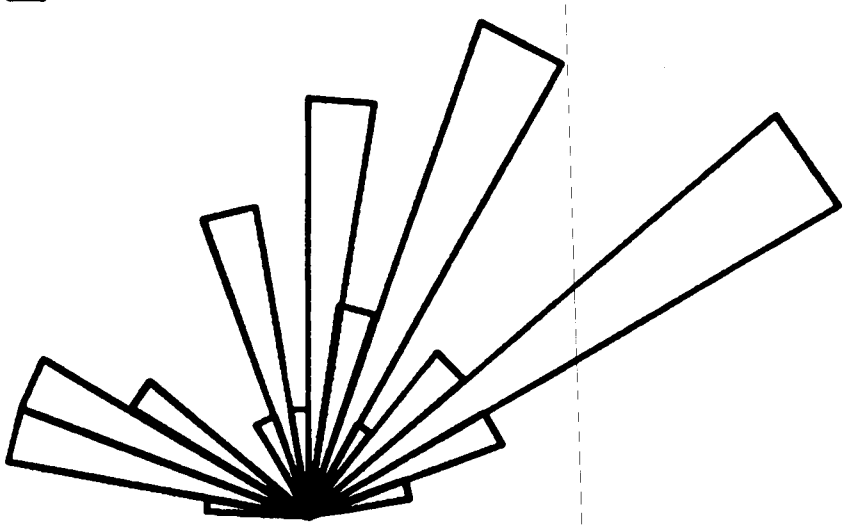
PHOTOGEOLOGIC LINEAR FEATURES



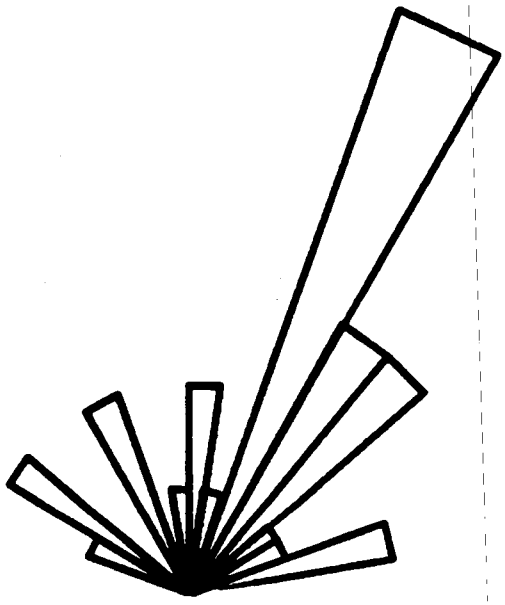
BEDROCK JOINTS

Figure B-11. Histogram of photogeologic linear feature orientations which lie within 1.5 miles of site K and histogram of joint orientations from field site K. North is at the top of the page. The top histogram is based on thirty-eight measurements and the bottom is based on twenty-five.

SITE L



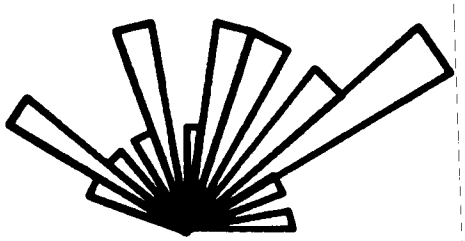
PHOTOGEOLOGIC LINEAR FEATURES



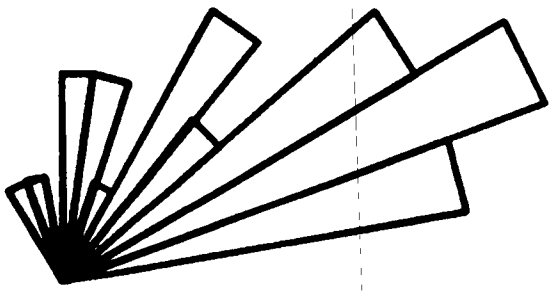
BEDROCK JOINTS

Figure B-12. Histogram of photogeologic linear feature orientations which lie within 1.5 miles of site L and histogram of joint orientations from field site L. North is at the top of the page. The top histogram is based on thirty-seven measurements and the bottom is based on twenty-five.

SITE N



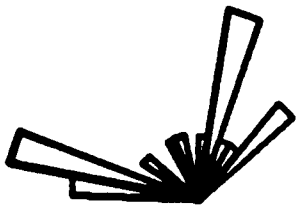
PHOTOGEOLOGIC LINEAR FEATURES



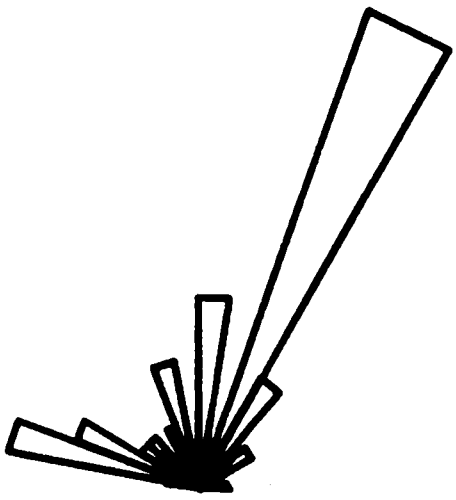
BEDROCK JOINTS

Figure B-13. Histogram of photogeologic linear feature orientations which lie within one mile of site N and histogram of joint orientations from field site N. North is at the top of the page. The top histogram is based on nineteen measurements and the bottom is based on twenty-five.

SITE O



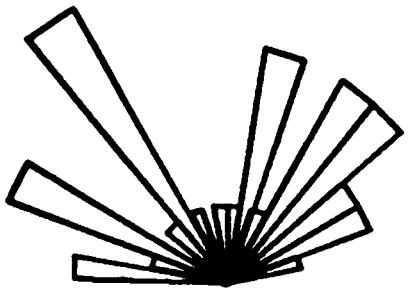
PHOTOGEOLOGIC LINEAR FEATURES



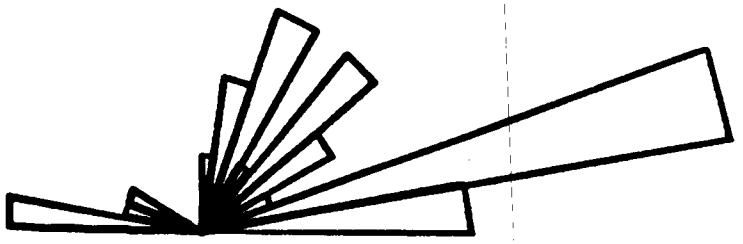
BEDROCK JOINTS

Figure B-14. Histogram of photogeologic linear feature orientations which lie within one mile of site O and histogram of joint orientations from field site O. North is at the top of the page. The top histogram is based on sixteen measurements and the bottom is based on twenty-five.

SITE P



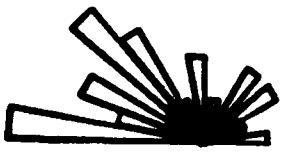
PHOTOGEOLOGIC LINEAR FEATURES



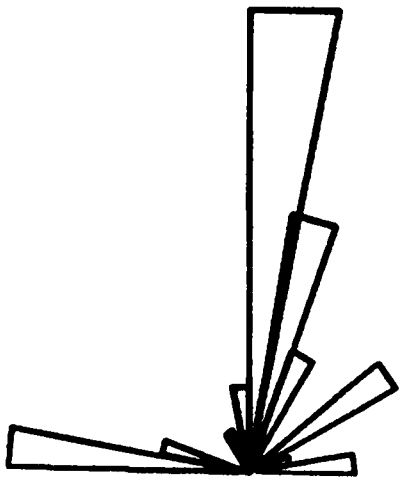
BEDROCK JOINTS

Figure B-15. Histogram of photogeoligic linear feature orientations which lie within 1.5 miles of site P and histogram of joint orientations from field site P. North is at the top of the page. The top histogram is based on twenty-nine measurements and the bottom is based on twenty-eight.

SITE Q



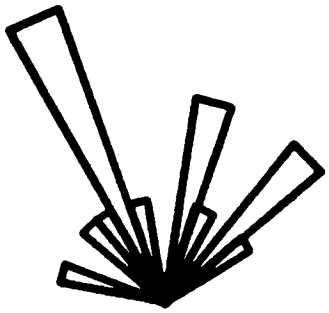
PHOTOGEOLOGIC LINEAR FEATURES



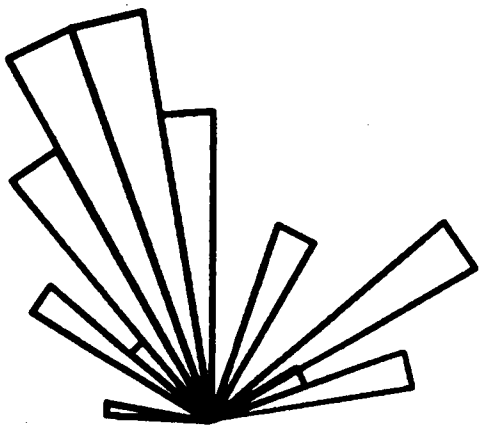
BEDROCK JOINTS

Figure B-16. Histogram of photogeologic linear feature orientations which lie within 1.5 miles of site Q and histogram of joint orientations from field site Q. North is at the top of the page. The top histogram is based on thirty measurements and the bottom is based on thirty-nine.

SITE R



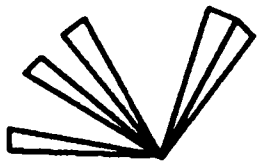
PHOTOGEOLOGIC LINEAR FEATURES



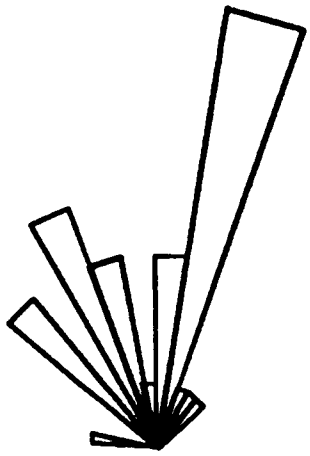
BEDROCK JOINTS

Figure B-17. Histogram of photogeologic linear feature orientations which lie within one mile of site R and histogram of joint orientations from field site R. North is at the top of the page. The top histogram is based on thirteen measurements and the bottom is based on twenty-six.

SITE S



PHOTOGEOLOGIC LINEAR FEATURES



BEDROCK JOINTS

Figure B-18. Histogram of photogeologic linear feature orientations which lie within 1.5 miles of site S and histogram of joint orientations from field site S. North is at the top of the page. The top histogram is based on twelve measurements and the bottom is based on twenty-five.

APPENDIX C

SUMMARY OF PHOTOGEOLOGIC DATA

Summary of All Photogeologic Linear Features Mapped in Project Area

Total number of photogeologic linear features mapped: 999

Linear features composed of a single photointerpretative element: 778 or 78% of total

Linear features composed of multiple photointerpretative elements: elements: 221 or 22% of total

Photogeologic Linear Features Composed of a Single Expression Element:

Soil: 0
Vegetation: 33 or 4% of total
Topographic-erosional: 745 or 96% of total

Photogeologic Linear Features Composed of Multiple Expression:

Soil + vegetation: 2 or .1% of total
Soil + topographic-erosional: 36 or 16% of total
Soil + vegetation + topographic-erosional: 4 or 2% of total
Vegetation + topographic-erosional: 179 or 81% of total

Continuity:

Continuous photogeologic linear features: 851 or 85% of total
Subcontinuous photogeologic linear features: 148 or 15% of total

Mappable Lengths:

Fracture traces less than one mile (1.61 kilometers): 927 or 93% of total
Lineaments greater than one mile (1.61 kilometers): 72 or 7% of total

Summary of Photogeologic Linear Features Mapped on ASCS Black and White Panchromatic Aerial Photographs

Total number of photogeologic linear features mapped: 966

Linear features composed of a single photointerpretative element: 751 or 78% of total

Linear features composed of multiple photointerpretative elements: 215 or 22% of total

Photogeologic Linear Features Composed of a Single Expression Element:

Soil: 0 or 0% of total
Vegetation: 33 or 4% of total
Topographic-erosional: 718 or 96% of total

Photogeologic Linear Features Composed of Multiple Expression Elements:

Soil + vegetation: 2 or .1% of total
Soil + topographic-erosional: 36 or 17% of total
Soil + vegetation + topographic-erosional: 4 or 2% of total
Vegetation + topographic-erosional: 173 or 80% of total

Continuity:

Continuous photogeologic linear features: 832 or 86% of total
Subcontinuous photogeologic linear features: 134 or 14% of total

Mappable Lengths:

Fracture traces less than one mile (1.61 kilometers): 906 or 94% of total

Lineaments greater than one mile (1.61 kilometers): 60 or 6% of total

Summary of Photogeologic Linear Features Mapped on NASA Color Infrared Imagery

Total number of photogeologic linear features mapped: 149

Linear features composed of a single photointerpretative element (topographic-erosional): 106 or 71% of total

Linear features composed of multiple photointerpretative elements (vegetation + topographic-erosional): 43 or 29% of total

Continuity:

Continuous photogeologic linear features: 111 or 75% of total

Subcontinuous photogeologic linear features: 38 or 25% of total

Mappable Lengths:

Fracture traces less than one mile (1.61 kilometers): 88 or 59% of total

Lineaments greater than one mile (1.61 kilometers): 61 or 41% of total

Linear features previously mapped on ASCS photographs: 116 or 78% of total

Linear features not previously mapped on ASCS photographs: 33 or 22% of total

VITA

Penny McFarlan Masuoka was born in Chattanooga, Tennessee, on October 15, 1955. She attended Hamilton County public schools and graduated from high school on June 1973. The fall of that year, she entered The University of Tennessee and received a Bachelor of Arts degree in the spring of 1977. That summer, she entered The University of Tennessee graduate school.